DEUTSCHES ELEKTRONEN-SYNCHROTRON DESY

DESY 83-096
Oktober 1983

THE DETERMINATION OF α_s IN e^+e^- ANNIHILATION

by

G. Wolf

Deutsches Elektronen-Synchrotron DESY, Hamburg

ISSN 0418-9833

NOTKESTRASSE 85 · 2 HAMBURG 52

To be sure that your preprints are promptly included in the
HIGH ENERGY PHYSICS INDEX ,
send them to the following address (if possible by air mail) :

DESY
Bibliothek
Notkestrasse 85
2 Hamburg 52
Germany

THE DETERMINATION OF α_s IN e^+e^- ANNIHILATION*

Günter Wolf

Deutsches Elektronen-Synchrotron, DESY
Hamburg, Germany

Abstract

The determination of α_s from nonresonant hadron production in e^+e^- annihilation is discussed. The measurements of $R = \sigma_{tot}/\sigma_{\mu\mu}$ yield $\alpha_s = 0.19 \pm 0.06$ in $O(\alpha_s^2)$ near $W = 34$ GeV. The error is dominated by experimental uncertainties. Studies of two- and three-jet production using event shapes and cluster properties in $O(\alpha_s^2)$ limit α_s to the range 0.15-0.22 at $W \approx 34$ GeV. The relatively large spread is caused by the lack of theoretical understanding of hadronization of quarks and gluons.

1. Introduction

Electron-positron collisions offer several ways to measure the strong coupling α_s. The majority of the experiments have focussed on e^+e^- annihilation into hadrons studying the total hadronic cross section, three-jet production or energy-energy correlations. An alternative is the comparison of the direct and the photonic decay modes of heavy quarkonia[1]. Eventually, the photon structure function extracted from two photon scattering may also provide a measurement of α_s[2].

This review reports on the results from the first three methods. The data discussed are those available at the time of the Lake Tahoe meeting plus some additional information presented at the conferences of the EPS in Brighton and of the Lepton-Photon Symposium in Cornell.

2. The total cross section

A precise measurement of the total cross section for e^+e^- annihilation into hadrons, σ_{tot}, offers a particularly clean test of QCD. Separation of the one-photon annihilation events from hadronic events produced by two-photon scattering, which becomes increasingly important as the energy increases, is straight forward. It is achieved by demanding that the observed hadron energy exceed a certain fraction of the total energy W. This cut eliminates also background from beam gas scattering. Contamination from τ-pair production is usually suppressed by a multiplicity and an effective mass cut. The acceptance efficiency of the high energy experiments is typically 70 - 80 % after all cuts are made. The luminosity is determined from small angle (few degrees)

* Talk given at the XIV International Symposium on Multiparticle Dynamics, Granlibakken, Lake Tahoe, USA, June 1983

DESY 83-096
Oktober 1983

ISSN 0418-9833

and/or large-angle Bhabha scattering, $e^+e^- \to e^+e^-$. Sizeable corrections have to be applied for radiative effects such as photon emission in the initial state, vertex corrections, and vacuum polarization[3].

The precision of most σ_{tot} measurements is determined by systematic uncertainties. Several groups measuring σ_{tot} at high energy have reported precision data with systematic errors near 3-5 %. At this level of accuracy the next order ($O(\alpha^4)$) QED radiative corrections become significant. They have not yet been calculated but are estimated at ~2 % of σ_{tot}.

Fig. 1 shows the total cross section in units of the high energy $O(\alpha^2)$ cross section for μ-pair production,

$$R = \sigma_{tot}/\sigma_{\mu\mu} \qquad (1)$$

$$\sigma_{\mu\mu} = 4\pi\alpha^2/3s \qquad (= \frac{87.6}{s}\text{nb},\ s = W^2 \text{ in GeV}^2)$$

where W is the total c.m. energy W. Included in Fig. 1 are the latest data from the PETRA experiments which extend the R measurements up to W = 43 GeV. The high precision high energy data are summarized in Table 1. For the determination of R the high energy region is of particular interest. As seen from Fig. 1 the data above W = 14 GeV are consistent with a constant R close to 4.0.

The QCD expression for R in second order is given by[4]

$$R = 3 \sum_q e_q^2 \left\{1 + \frac{\alpha_s}{\pi} + C_2 \left(\frac{\alpha_s}{\pi}\right)^2\right\} \qquad (2)$$

where e_q is the quark charge and $C_2 = 1.99 - 0.12 \cdot N_f$ (N_f = number of quark flavours) in the $\overline{MS}$ scheme. The lowest order QCD diagrams are depicted in Fig. 2. For $\alpha_s = 0.2$ the higher order QCD corrections present an increase of R by ~7 %. At the high energies now available, the contribution from Z^0 exchange[5] has to be taken into account. For instance at W = 30 GeV it amounts to +1.2 % assuming $\sin^2\theta_W = 0.23$ and the predictions of the standard theory for the weak couplings. Corrections for finite quark masses have been calculated for R and α_s [6]. In the region of interest they change R by less than 1 % and reduce α_s by 10 - 15 %. Taking this correction and the Z^0 contribution into account the data[7] yield the α_s values shown in the last column of Table 1.

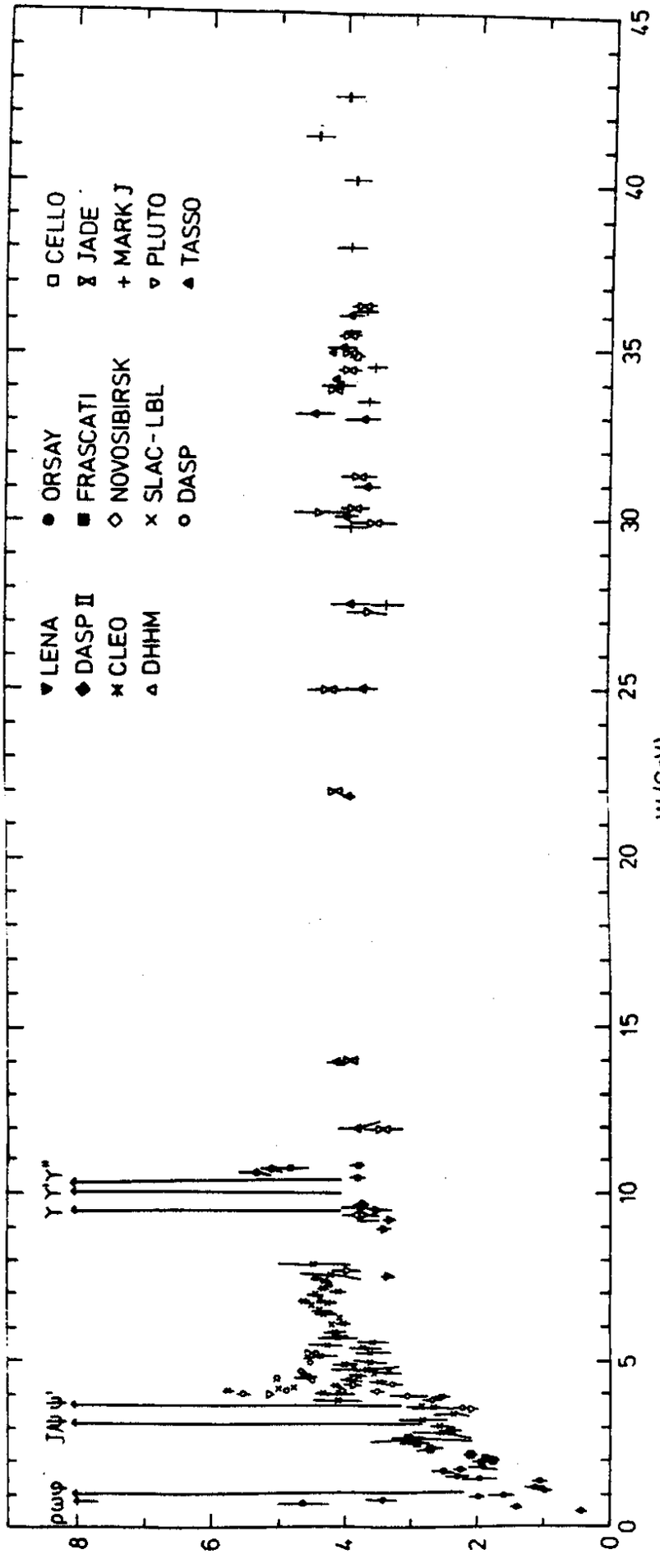

36341

Fig.1 The ratio R of the total cross section for e^+e^- annihilation into hadrons to the μ pair cross section, $\sigma_{\mu\mu} = 4\pi\alpha^2/3s$.

Table 1: Summary of high energy R measurements[7]. Only R values averaged over the W range indicated are given. Also given is α_s deduced by the author from the R values correcting for the Z^0 contribution and for quark mass effects

Experiment	W (GeV)	$R \pm \Delta R_{stat} \pm \Delta R_{syst}$	$\alpha_s \pm \Delta\alpha_s$ stat $\pm \Delta\alpha_s^*$ syst
TASSO	30-36.7 (average 34.4)	4.05±0.06±0.19*	0.24±0.04±0.13
JADE	30-36.7 (average 34.4)	3.99±0.04±0.10	0.20±0.03±0.08
MARK J	30-36.7 (average 34.4)	3.95±0.05±0.22	0.18±0.03±0.15
MARK II	29.0	3.90±0.05±0.25	0.17±0.03±0.17
MAC	29.0	3.87±0.10±0.10	0.15±0.06±0.08

* The systematic error includes a 2 % uncertainty to account for the unknown second order corrections.

The weighted average is

$$\alpha_s(s = 1170\ \text{GeV}^2) = 0.19 \pm 0.06$$

where the error is dominated by the systematic uncertainties.

3. Three-jet production

At high energies ($W \gtrsim 30$ GeV) roughly 5-10 % of the hadronic events in e^+e^- annihilation show a definite three-jet structure[8]. The prediction of such events is one of the great successes of QCD which explains them as a result of hard gluon bremsstrahlung[9,10]. In lowest order this leads to the process (see diagrams b, c in Fig. 2)

$$e^+e^- \to q\bar{q}g \ .$$

Denoting by x_1 and x_2 the fractional energies of the quarks, $x_i = 2E_i/W$, the cross section for gluon emission is given by[10]

$$\frac{d\sigma(q\bar{q}g)}{dx_1 dx_2} = \frac{2\alpha_s}{\pi}\ \sigma_o \frac{x_1^2 + x_2^2}{(1-x_1)(1-x_2)} \qquad (3)$$

where $\sigma_o = 3\sigma_{\mu\mu}\ \Sigma e_q^2$. The event structure at the parton level is completely defined by x_1 and x_2; e.g. the angles Θ_i between the three partons (see Fig. 3) are related to the x_i by

$$x_i = \frac{2\sin\Theta_i}{\sin\Theta_1 + \sin\Theta_2 + \sin\Theta_3} \qquad i = q,\bar{q},g \qquad (4)$$

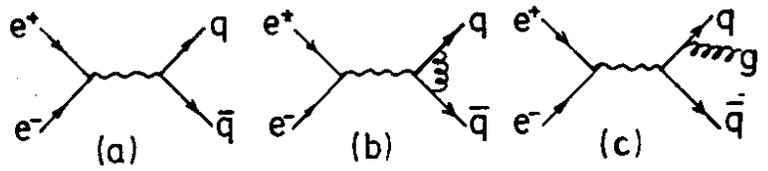

Fig.2 Quark parton diagram and lowest order QCD diagrams for $e^+e^- \to q\bar{q}$.

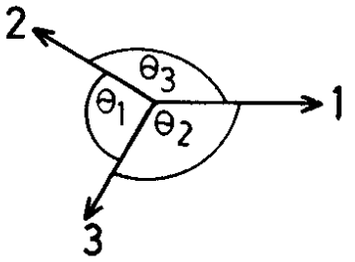

Fig.3 $q\bar{q}g$ state

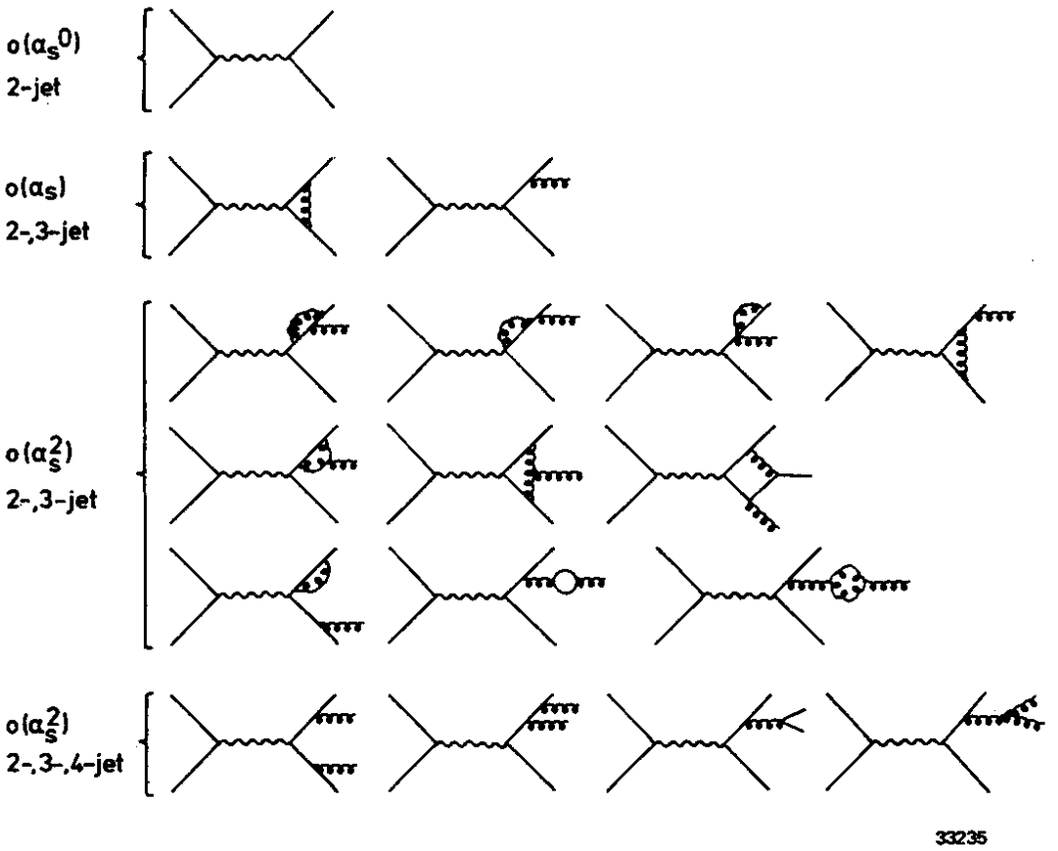

Fig.4 QCD diagrams for e^+e^- → hadrons

The cross section for $q\bar{q}g$ production is directly proportional to α_s. However, the QCD prediction is made at the parton level. In order to compare it with the data one has to combine the QCD calculation with a model that describes quark and gluon fragmentation into hadrons. Using the QCD models of Hoyer et al.[11] or of the Lund group[12] QCD was found to reproduce the relevant data such as the distribution of the jet energies x_i or of the jet angles Θ_i and the W dependence of three-jet production. It could also been shown that the data are consistent with spin one for the gluon as predicted by QCD while they exclude scalar gluons[13].

Several models have been proposed which maintain that three-jet events are not necessarily due to gluon bremsstrahlung but can be explained by a different mechanism, such as

i) pure $e^+e^- \to q\bar{q}$ production with an exponential or power tail for the quark fragmentation into hadrons.

ii) pure $e^+e^- \to q\bar{q}$ production with a Gaussian p_T distribution, $\sim\exp(q_T^2/2\sigma_q^2)dq_T^2$, but with different values of σ_q for light and heavy quarks.

iii) hard emission of a meson or meson system as described by the constituent interchange model[14] (CIM).

A detailed comparison with experiment has shown that none of these models can explain all features of the data[15].

Geometrodynamics has been proposed as yet another alternative to QCD[16]. The model seems to reproduce the data. It treats hadron production from the beginning at the hadron level. A hard branching process is introduced which leads e.g. to the three-jet events. It has been argued[17] that such a branching process can only occur as the result of the hard emission of a field quantum. In this case the branching process might be a model of gluon emission described with physical states (i.e. at the hadron level).

3.1 Second order corrections

QCD predictions in second order α_s for jet production have first been presented by Ali et al.[18]. These included the diagrams leading to $q\bar{q}gg$ and $q\bar{q}q\bar{q}$ final states. Complete (apart from virtual corrections to $e^+e^- \to q\bar{q}$) second order calculations including the virtual corrections to to $e^+e^- \to q\bar{q}g$ (see Fig. 4) have been carried out by ERT[19], FKSS[20] and VGO[21], with conflicting results. In the case of ERT and VGO the $O(\alpha_s^2)$ corrections have been large whereas FKSS have found them small. At the origin of the discrepancy is the use of different definitions for when two partons i and j are called two separate jets. Denote y_{ij} as the scaled invariant mass squared of partons i and j,

$$y_{ij} = M_{ij}^2/W^2 \qquad (5)$$

then VGO have considered i and j as two separate jets if $y_{ij} > y = 10^{-5}$ for W = 30 GeV (or $M_{ij} > 0.1$ GeV). This is an extremely small cut-off compared to the mass of a single quark jet which is typically several GeV. Fig. 5 shows the 3- and 4-jet cross sections at the parton level and their sum as a function of the cutoff y. For $y < 0.014$ the 3-jet cross section is negative, for $y < 0.004$ even the sum of the 3- and 4-jet cross sections is negative. This indicates that at y values as small as that higher order corrections (beyond $O(\alpha_s^2)$) become important. For a detailed discussion see Ref. 23.

FKSS have used a Sterman-Weinberg type jet definition: two partons are counted as two separate jets if either energy is bigger than $\varepsilon W/2$ and the angle between them is bigger than δ. A reasonable set of (ε,δ) values is $(0.2, 40^o)$ which at W = 30 GeV corresponds roughly to a y cut of 0.025 (0.013) for a 3- (4-) parton state. With this choice of cutoff parameters the 4-jet cross section is small and the $O(\alpha_s^2)$ correction to the 3-jet cross section is small as well. This is achieved at the cost of neglecting soft partons (with energy less than $\varepsilon W/2$ emitted outside of the cones of the energetic partons[24]). A further approximation made by FKSS is the neglect of $O(\varepsilon,\delta)$ terms. It has been argued that for (ε,δ) as large as $(0.2, 40^o)$ these terms are nonnegligible.

3.2 Fragmentation models

a) Independent jet fragmentation

The first determinations of α_s have used the models of Hoyer et al.[11] (which includes only terms of $O(\alpha_s)$) and of Ali et al.[18] (which includes all second order 4-parton diagrams but not the virtual corrections). In both models quarks and gluons fragment independently (see Fig. 6). As a result the momentum vectors of the jets on average reproduce faithfully the directions of the primary partons.

The fragmentation of quarks and gluons into hadrons follows the Field-Feynman scheme[25]:

1) The fragmentation function f(z) for $q \to q' + h$ is taken to be

$$f(z) = 1-a_F + 3a_F(1-z)^2, \quad z = \frac{(p_{||}+E)_h}{(p_{||}+E)_q} \tag{6}$$

The fragmentation process is recursive and is repeated until the energy of the remaining quark is zero.

2) The distribution of the transverse momentum q_T of the quarks in the jet cascade is $\sim\exp(-q_T^2/2\sigma_q^2)dq_T^2$.

3) Only pseudoscalar $(\pi,K,...)$ and vector mesons $(\rho,K^*,...)$ are assumed to be produced. The relative production rate in the primordial cascade is described by the ratio P/(P+V).

4) The production ratio of strange to nonstrange $q\bar{q}$ pairs from the vacuum is given by P(s)/P(u) = P(s)/P(d).

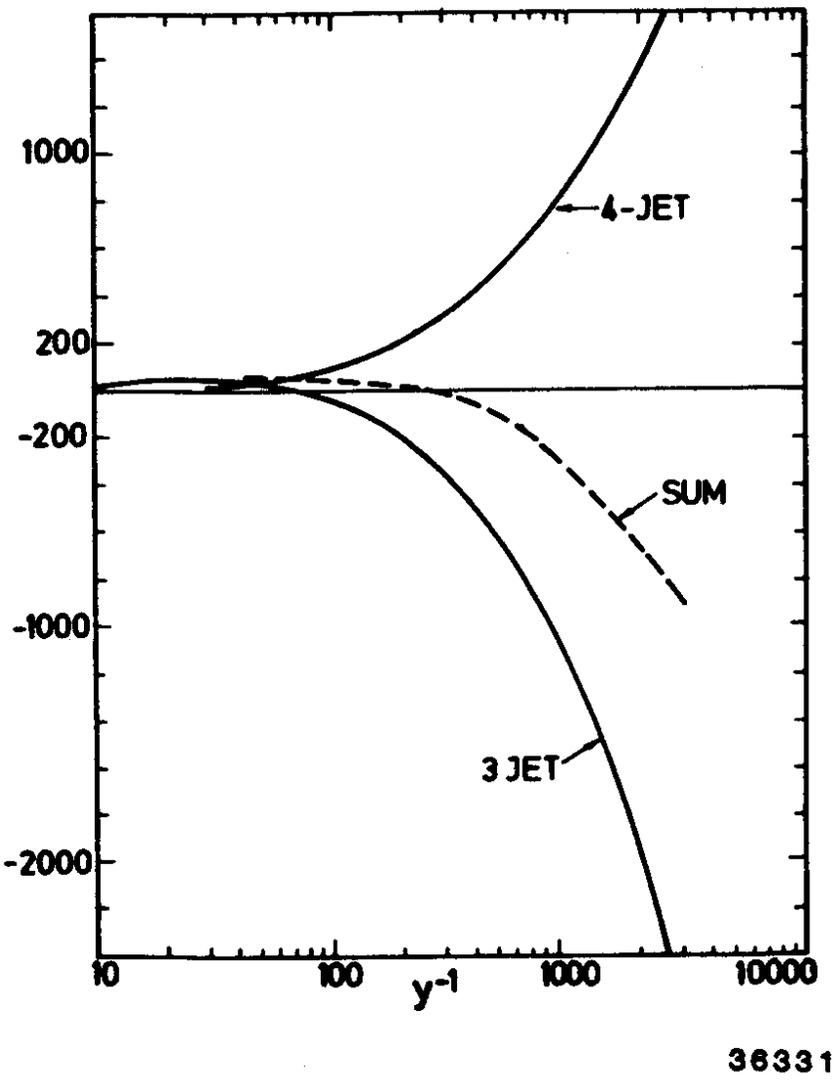

Fig.5 Integrated 3 and 4 jet cross sections calculated from QCD at the parton level. From Ref. 23.

b) String fragmentation

In the model of the LUND group[12] the coloured partons are connected by colour field lines (strings) which break up to form hadrons. The main difference to the independent jet models shows up in the fragmentation of events containing one or more gluons. In the case of $e^+e^- \to q\bar{q}g$ the gluon generates a kink in the string stretched between q and $\bar{q}$. The string breaks, at the gluon corner, into two $q\bar{q}$ pairs $(q_1\bar{q}_1)(q_2\bar{q}_2)$ from which a leading hadron composed of $q_1\bar{q}_2$ is formed (Fig. 7a). The two left-over string pieces $(q\bar{q}_1)$ and $(q_2\bar{q})$ fragment into hadrons in their own rest frames. In the total c.m. system the resulting jet momentum vectors in general do not reproduce the directions of the primary partons (Fig. 7b). Qualitatively speaking, the angle between the gluon jet and the nearest quark jet is smaller than at the parton level. As a result a $q\bar{q}g$ event after fragmentation in the Lund model is less three-jet like than in the independent jet model.

We shall refer to the Lund model as the string model.

3.3 Measures for three-jet production

The procedure followed to determine α_s has been either to study event shapes or to isolate genuine three-jet events with a cluster algorithm[26].

a) event shape analysis

A basic tool in the event shape analyses has been the momentum tensor[27],

$$M_{\alpha\beta} = \sum_{j=1}^{N} p_{j\alpha} p_{j\beta} \Big/ \sum_{j=1}^{N} p_j^2 \qquad (\alpha,\beta = x,y,z) \tag{7}$$

Diagonalization yields the unit eigenvectors $\hat{n}_1$, $\hat{n}_2$, $\hat{n}_3$ and the corresponding eigenvalues

$$Q_k = \sum (p_j \cdot n_k)^2 / \sum p_i^2 \quad . \tag{8}$$

The Q_k satisfy the relation

$$Q_1 + Q_2 + Q_3 = 1 \tag{9}$$

If they are ordered such that $Q_1 < Q_2 < Q_3$ they measure the flatness (Q_1), the width (Q_2) and the length (Q_3) of an event. The plane spanned by $\hat{n}_2$ and $\hat{n}_3$ is the event plane and $\hat{n}_3$ is the jet axis (see Fig. 8). The Q_k can be expressed in terms of the momentum components out of and in the event plane, $p_{T\,out} = |\vec{p}_j \cdot \hat{n}_1|$, $p_{T\,in} = |\vec{p}_j \cdot \hat{n}_2|$:

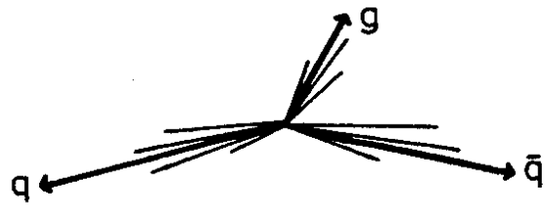

Figs.6 A $q\bar{q}g$ event in the independent jet fragmentation model

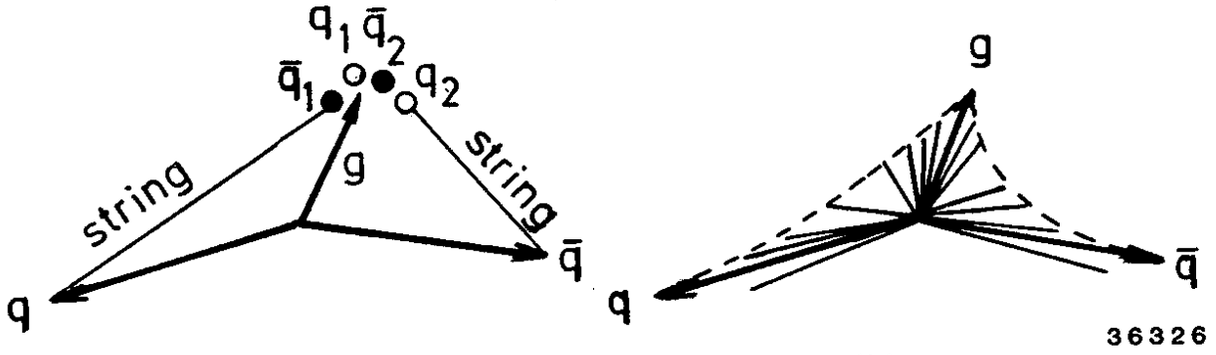

Fig.7 A $q\bar{q}g$ event in the string model

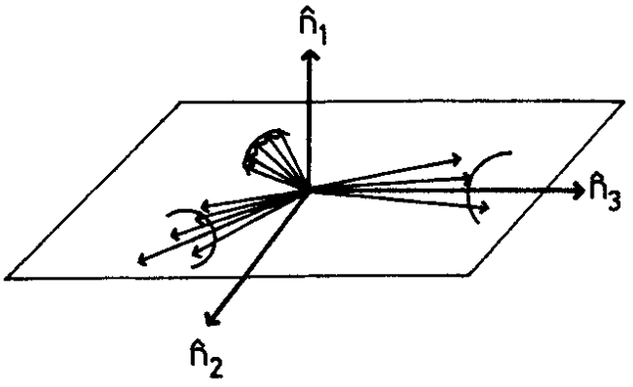

Fig.8 The coordinate system determined for a three-jet event by the momentum tensor

$$Q_1 = \langle p_{T\ out}^2 \rangle / \langle p^2 \rangle$$
$$Q_2 = \langle p_{T\ in}^2 \rangle / \langle p^2 \rangle \qquad (10)$$

where the average is taken over the particles of an event. The sphericity (S) and aplanarity (A) are given by

$$S = 3/2(Q_1 + Q_2) = 3/2(1 - Q_3)$$
$$A = 3/2\ Q_1 \qquad (11)$$

The jet measures derived from the momentum tensor are weighted quadratically by the particle momenta. Linear weighting is provided by using the thrust T, major and minor axes, defined as

$$T = \text{Max}\ (\Sigma|p_j \cdot \hat{n}_3|/\Sigma p_j) \qquad (12)$$

The major axis $\hat{n}_2$ is perpendicular to $\hat{n}_3$ and is the direction along which the projected momentum flow in the plane perpendicular to $\hat{n}_3$ is a minimum

$$\text{Major} = \text{Max}\ (\Sigma|p_j \cdot \hat{n}_2|/\Sigma p_j) \qquad (13)$$

Accordingly, $\hat{n}_1 = \hat{n}_2 \times \hat{n}_3$ and

$$\text{Minor} = \Sigma|p_j \cdot \hat{n}_1|/\Sigma p_j \qquad (14)$$

The difference = = Major - Minor is called the oblateness.

It has been stressed by Clavelli[28] that the effective masses of jets are a sensitive measure of gluon emission. Each event is divided into two hemispheres by a plane perpendicular to the jet axis $\hat{n}_3$. The higher (lower) jet mass in the event is denoted by M_H (M_L). The variable used is the normalized difference

$$\Delta M^2 = \frac{M_H^2 - M_L^2}{W^2} \qquad (15)$$

We conclude with a remark on the correlation between fragmentation effects and the value of α_s. Three-jet events are characterized by hadrons of large transverse momenta in the event plane (Fig. 8). Fragmentation and the decays of heavy quarks in genuine $q\bar{q}$ events contribute also to large p_T hadrons leading to a correlation between α_s and the fragmentation parameters. However, the large p_T hadrons from $q\bar{q}$ events are not restricted to lie in the event plane and therefore an analysis of the p_T distribution in and out of the event plane allows to separate fragmentation effects from those of gluon bremsstrahlung. In the same vein, $q\bar{q}g$ contributions affect the shape of the sphericity distribution while that of the aplanarity distribution is hardly changed.

b) cluster analysis

The cluster search of Daum et al.[26] has been used to find jets. The search is performed in several steps:

1) Group particles into clusters with half-cone angle α.

2) Order the clusters according to their energies, $E_1 > E_2 > \ldots > E_n$.

3) Remove all m low energy clusters which satisfy

$$\sum_{k=n-m+1}^{n} E_k < \varepsilon W/2 \ .$$

4) Keep only jets with $E_j > E_0$.

Typical parameter values used in the search are $\alpha = 30^0$, $\varepsilon = 0.1$ and $E_0 = 2$ GeV. For the α_s analysis events with three clusters are used. A typical three jet event is shown in Fig. 9.

3.4 Determination of α_s

The first determinations of α_s have been carried out in 1979/80 with typically a thousand hadronic events per experiment at c.m. energies near W = 30 GeV. The results are listed in Table 2. All analyses used the independent jet model.

Table 2: Early measurements of α_s. The first error for α_s is statistical, the second systematic.

Group	distributions fitted	fit parameters	QCD model	QCD correction	α_s
MARK J	oblateness	σ_q, α_s	Ali et al.	incomplete $O(\alpha_s^2)$	$0.23\pm0.02\pm0.04$ [29] $0.19\pm0.02\pm0.04$ [30]
TASSO	dN/dx_p, $\langle p^2_{\text{tout}} \rangle$, S, A	a_F, σ_q, P/P+V, α_s	Hoyer et al.	$O(\alpha_s)$	$0.19\pm0.02\pm0.03$
			Ali et al.	incomplete $O(\alpha_s^2)$	$0.17\pm0.02\pm0.03$ [31]
JADE		α_s	Hoyer et al.	$O(\alpha_s)$	$0.18\pm0.03\pm0.03$ [32]
PLUTO	3-cluster events, parton thrust x_1	α_s	Hoyer et al.	$O(\alpha_s)$	$0.15\pm0.03\pm0.02$ [33]

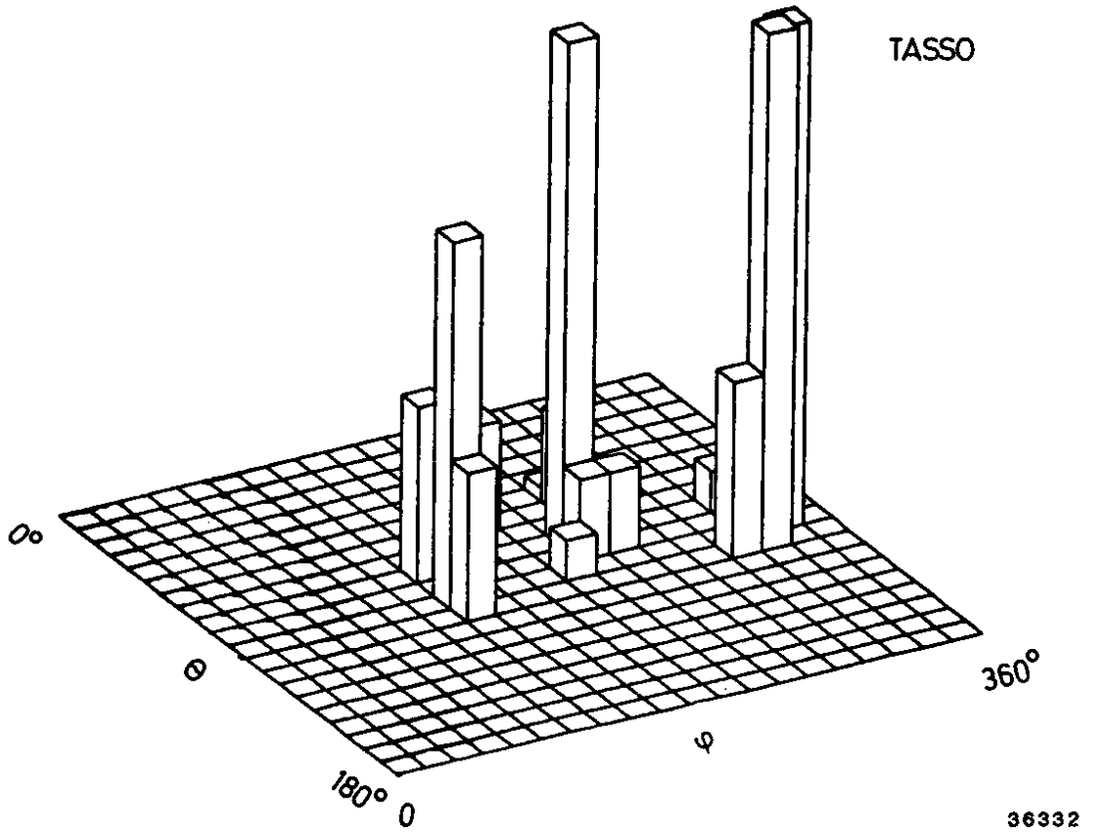

Fig.9 A typical three jet event

Table 2 yields as an average value

$$\alpha_s = 0.19 \pm 0.02 \pm 0.03 \quad \text{in } O(\alpha_s)$$
$$= 0.17 \pm 0.02 \pm 0.03 \quad \text{in (incomplete) } O(\alpha_s^2) \ .$$

Last year the CELLO group[34] presented an analysis where α_s has been extracted from the data using the independent-jet (Hoyer et al.) as well as the string fragmentation schemes (Lund model). The parton level cross section was calculated in first order QCD. The analysis was based on ~3000 hadronic events and a variety of shape measures as well as cluster properties have been studied. Figs. 10-12 show comparisons of the distributions of aplanarity, thrust, $p_{T\ in}$, $p_{T\ out}$, and cluster thrust with the Monte Carlo predictions for both fragmentation models.

Some of the CELLO results for α_s are given in Table 3.

Table 3: Determination of α_s in $O(\alpha_s)$ by the CELLO group[34]

distributions fitted	α_s independent jet	string
fraction of events with $S > 0.25$, $A < 0.1$	0.19 ± 0.03	0.28 ± 0.045
fraction of events with $O > 0.2$	0.19 ± 0.02	0.26 ± 0.04
3-cluster events	0.145 ± 0.02	0.235 ± 0.025
parton thrust x_1	0.155 ± 0.015	0.235 ± 0.025

The important conclusion from Table 3 is that the two fragmention schemes lead to different values of α_s, the string result being ~40 % larger than α_s determined with independent jets.

The JADE group[35] using 4800 events has presented a similar study for cluster properties in first and second order QCD, the latter using the complete second order corrections of FKSS. Fig. 13 shows the distributions of parton thrust, x_1 and of x_T, the fractional transverse momentum of parton 2, $x_T = x_2 \sin\Theta_3$, where Θ_3 is the angle between the partons 1 and 2. The solid lines show the $O(\alpha_s^2)$ QCD prediction for $\alpha_s = 0.16$, the dashed lines give the $O(\alpha_s)$ prediction for the same value of α_s. The difference between the first and second order calculations is ~20 % and hence small. The JADE group has concluded that independent jet and string fragmentation models within errors yield the same value for α_s,

$$\alpha_s = 0.20 \pm 0.015 \pm 0.03 \quad \text{in } O(\alpha_s)$$
$$= 0.16 \pm 0.015 \pm 0.03 \quad \text{in } O(\alpha_s^2) \ .$$

Taken at face value the JADE conclusion is at variance with the findings of CELLO. On the other hand, the upper end of α_s values allowed

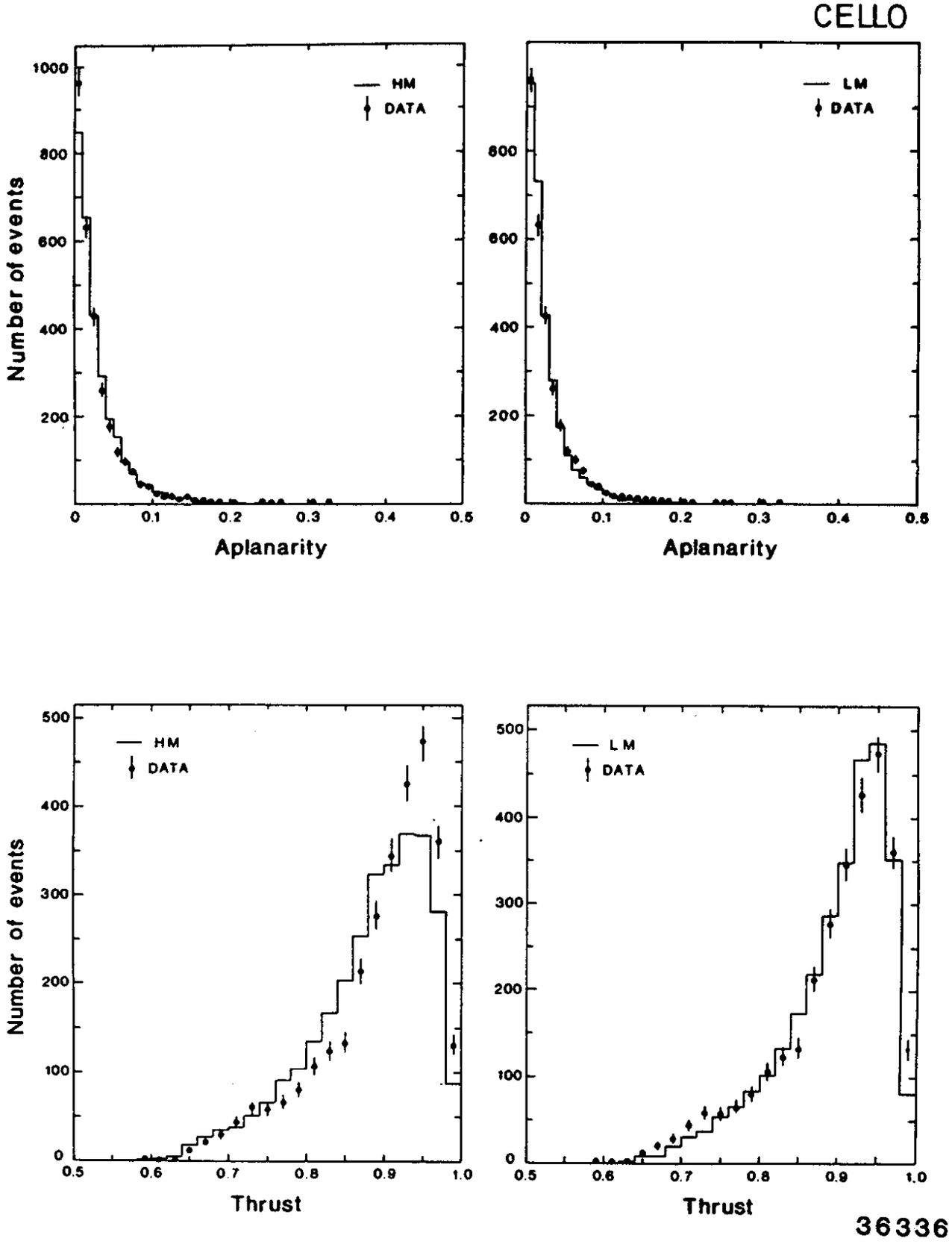

Fig.10 The measured aplanarity and thrust distributions (•) compared with QCD models in $O(\alpha_s)$ using independent jet (HM) and string fragmentation (LM). From CELLO, Ref. 34.

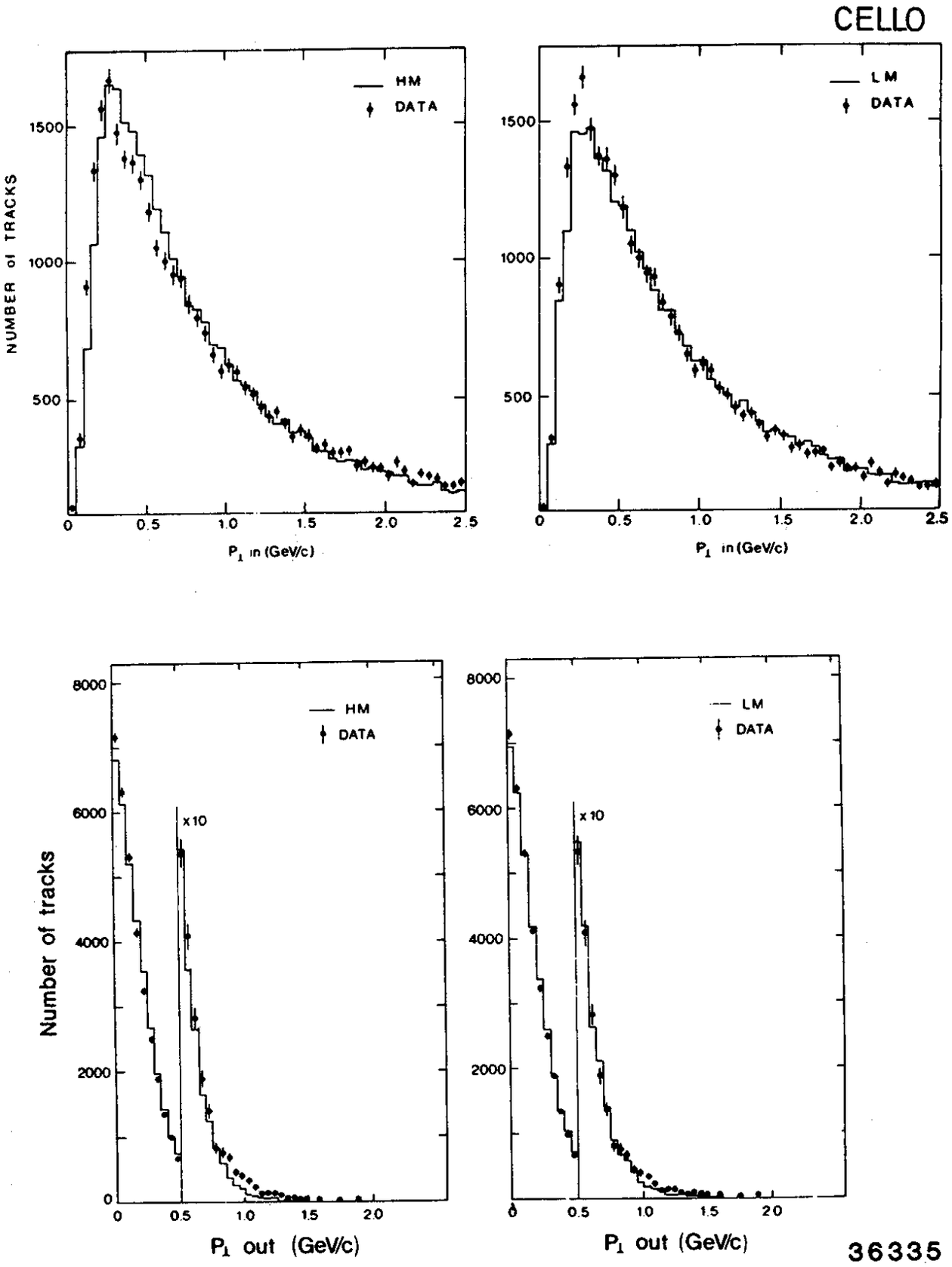

Fig.11 The measured p_{Tin} and p_{Tout} distributions (•) compared with QCD models in $O(\alpha_s)$ using independent jet (HM) and string fragmentation (LM). From CELLO, Ref. 34.

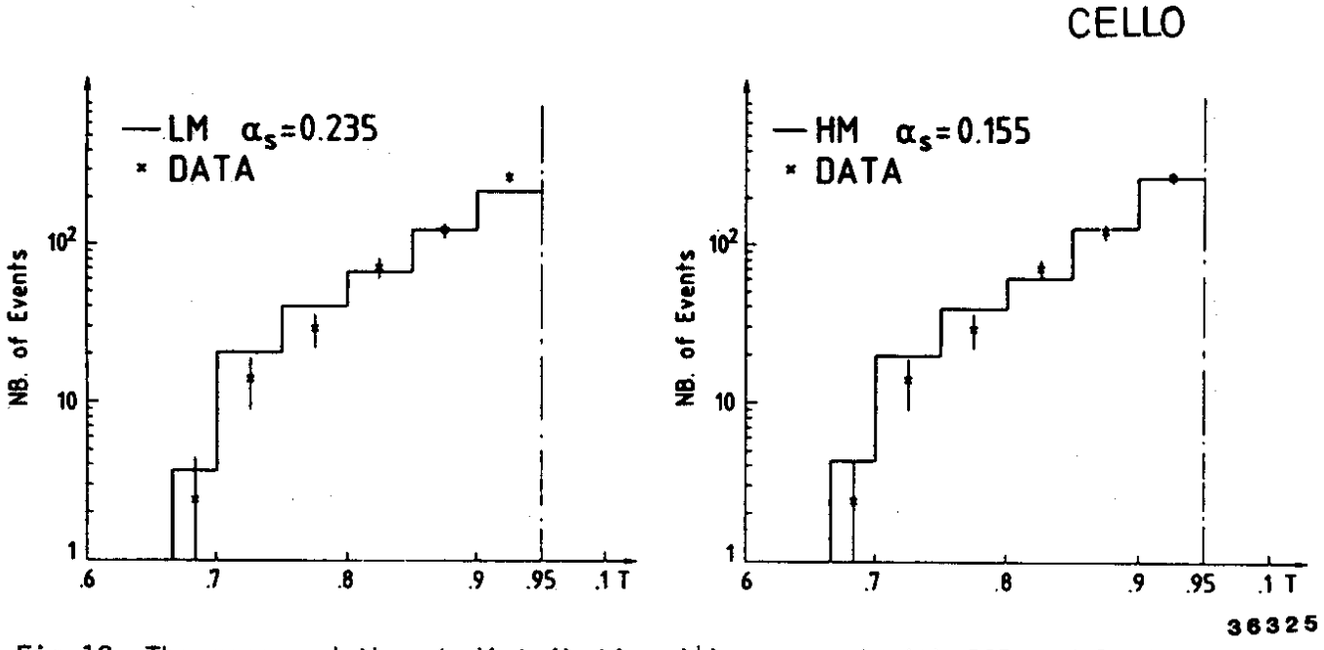

Fig.12 The measured thrust distribution (•) compared with QCD models in $O(\alpha_s)$ using independent jet (HM) and string fragmentation (LM). From CELLO, Ref. 34.

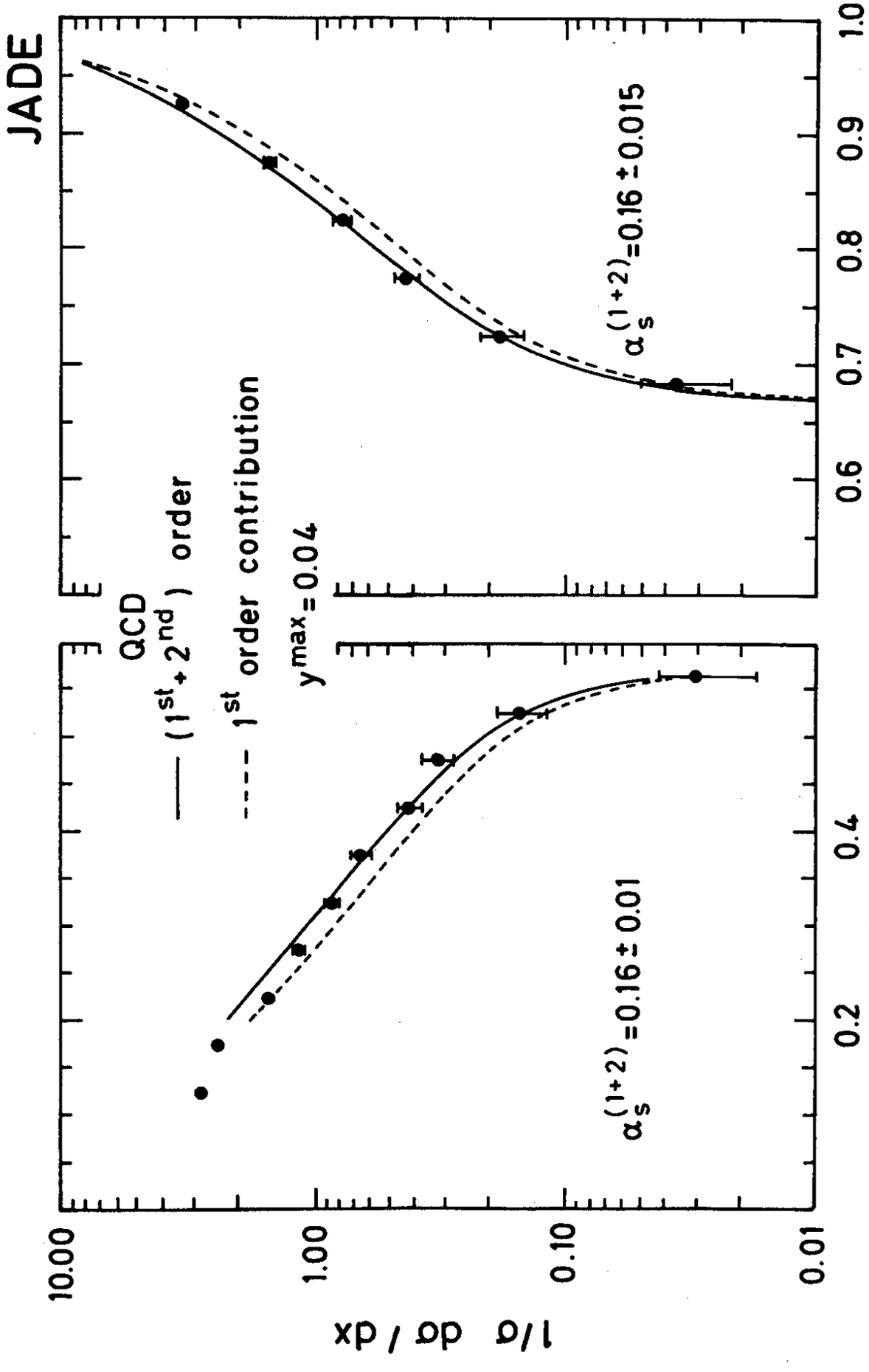

Fig.13 Corrected distributions of x_1 (= fractional energy of the most energetic jet) and of $x_\perp$ (= fractional transverse energy of the second jet) compared with the QCD model predictions in $O(\alpha_s)$ and $O(\alpha_s^2)$. From JADE, Ref. 35.

by JADE agrees with the string result of CELLO while the lower end of JADE's α_s values agrees with the independent jet result of CELLO.

In their fits for α_s, neither CELLO nor JADE have optimized the fragmentation parameters and one may wonder, e.g. to what extent the discrepancies observed in the CELLO analysis between independent-jet model and data for thrust (Fig. 10) and $p_{T\ in}$ (Fig. 11) affect their conclusion on the model dependence of α_s. This limitation has been avoided in the recent TASSO analysis[36] by fitting simultaneously α_s and the fragmentation parameters.

The TASSO analysis is based on 16 000 hadronic events. A Monte Carlo event generator has been written to calculate the second order QCD parton level cross sections according to FKSS. Fragmentation of quarks and gluons has been calculated in the independent jet and the string models. The measured inclusive cross sections on π^+, π^0, K^+, K^0, ρ^0, K^*, D^{*+}, p, Λ and Ξ^- production have been used in the determination of the fragmentation parameters. Figs.14 and 15 show the type of agreement reached between data and QCD model for inclusive K^0,$\overline{K^0}$, Λ,$\bar{\Lambda}$, $\pi^\pm$, $K^\pm$ and p,$\bar{p}$ production.

For the fragmentation function of u, d and s the following form has been employed (in independent jet and string fragmentation):

$$f(z) = (1 + a_L)(1 - z)^{a_L} \tag{16}$$

This form[12] has been found to give a better description of the charged particle momentum spectrum than the original from (eq.(6)) suggested by Field-Feynman. c and b quark fragmentation has been described by the form introduced by Peterson et al.[37]:

$$f(z) \sim \frac{1}{z(1 - \frac{1}{z} - \frac{\varepsilon}{1-z})^2} \tag{17}$$

with $\varepsilon = 0.18$ for c as determined from $D^\pm$ production[38] and $\varepsilon = 0.04$ for b as measured from the lepton spectra[39]. For the pseudoscalar/vector ratio a value of $P/(P+V) = 0.42$ determined from $\pi^\pm$ and ρ^0 production[40], has been used. The $\pi^\pm$, $K^\pm$ and K^0, $\overline{K^0}$ data[41] yield $P(s)/P(u) = P(s)/P(d) = 0.4$. The P, Λ[41] and Ξ[42] data have been used to adjust the amount of baryon production. The relative probability for baryon emission[43],

$$P_{baryon} = \frac{P(q \to q' + \text{Baryon})}{P(q \to q' + \text{meson}) + P(q \to q' + \text{Baryon})} \tag{18}$$

for the independent jet model has been set to 0.11. In a similar way the baryon parameters in the string model have been chosen.

Fits have been performed to the total event sample. The correlations between α_s and fragmentation parameters has been taken into account by simultaneously fitting a_L, σ_q and α_s. The fits have been done with several combinations of (corrected) event shape distributions.

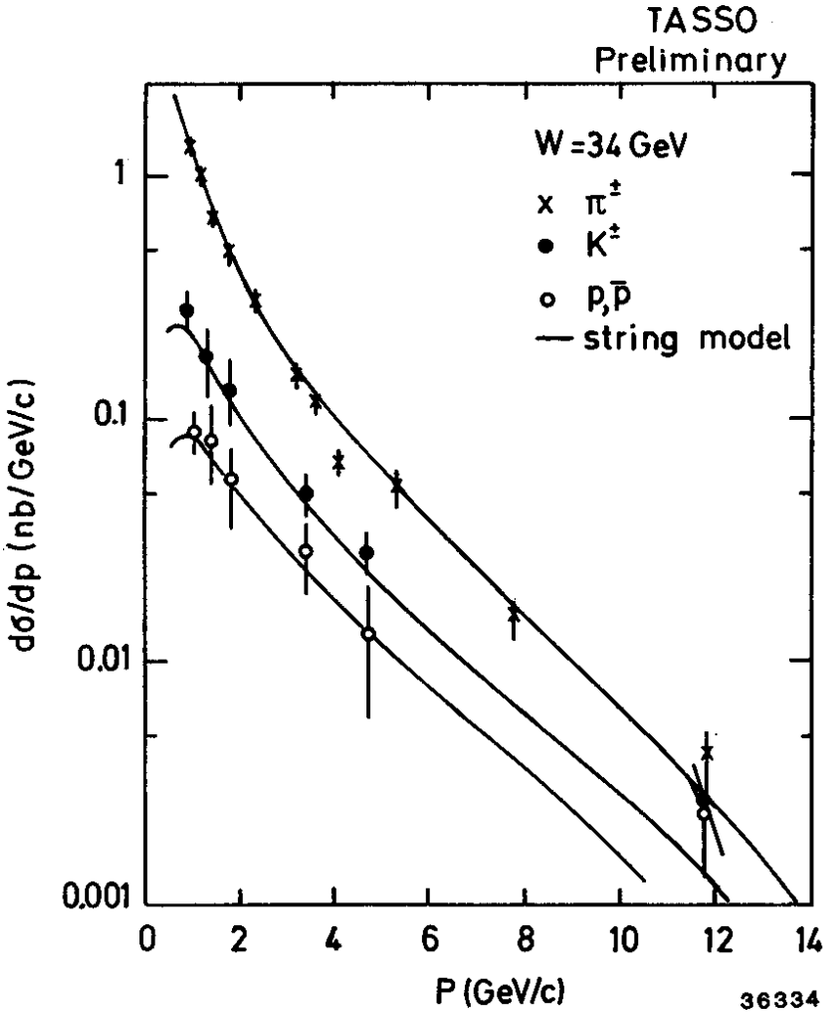

Fig.14 The inclusive momentum spectra for $\pi^+ + \pi^-$, $K^+ + K^-$ and $p + \bar{p}$ compared with QCD using the string model. From TASSO, Ref. 36.

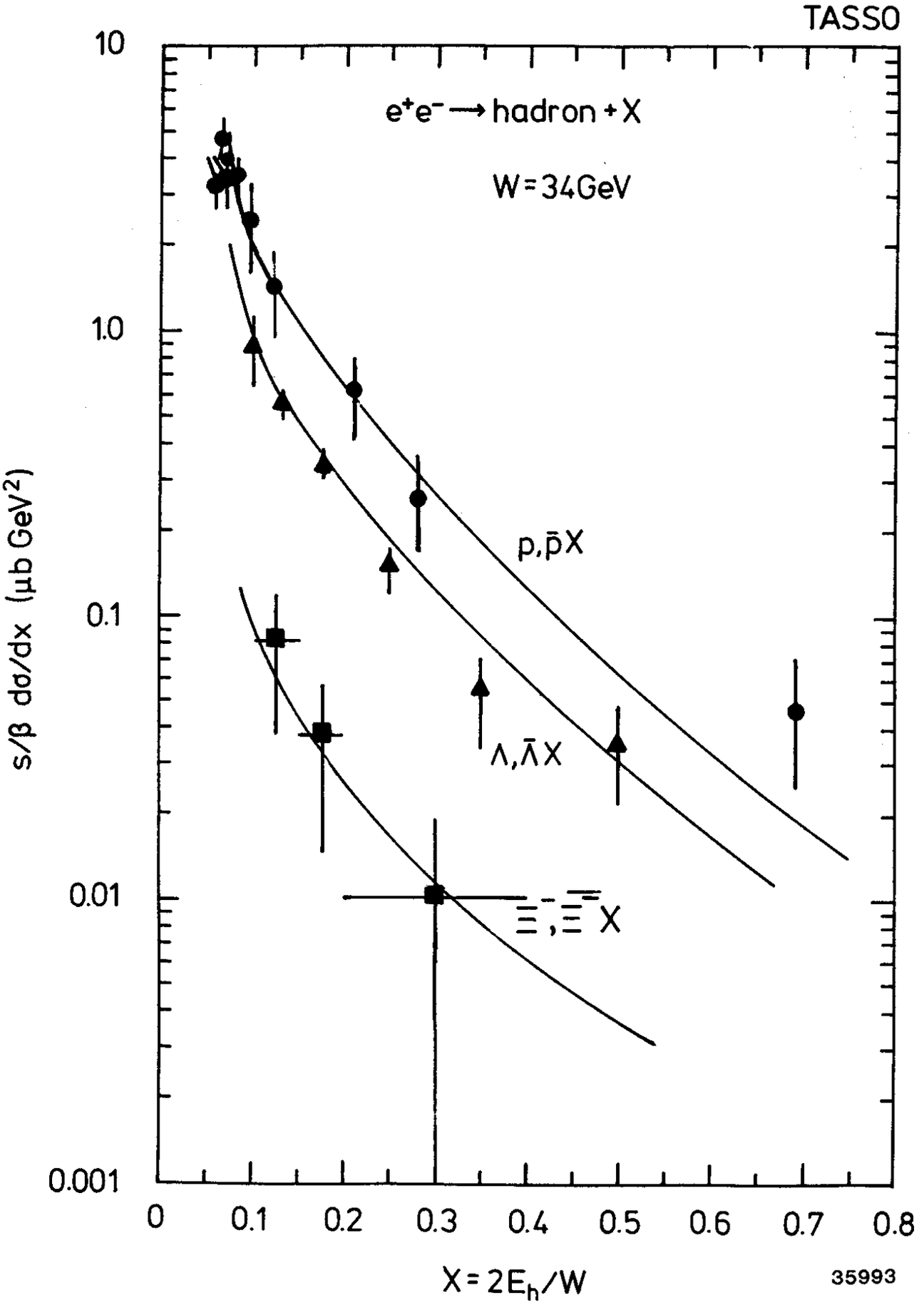

Fig.15 The scaled cross sections for $p + \bar{p}$, $\Lambda + \bar{\Lambda}$ and $\Xi^- + \overline{\Xi^-}$ production compared with QCD using string fragmentation. From TASSO.

Some of the fit results obtained for first and second order QCD with independent jet and with string fragmentation are listed in Tables 4, 5 and Figs. 16-19. In the tables are also indicated the combinations of distributions used in the fits. x_p is the fractional momentum of a charged particle, $x_p = 2p/W$. The corresponding distribution fitted is $1/\sigma_{tot}\, d\sigma/dx_p$. For each of the combinations the first distribution is particularly sensitive to a_L, the second to σ_q, and the perturbative tail of the third to α_s.

Table 4a: Fit results for the independent jet model, 1st order QCD (from TASSO[36]).

Distribution			a_L	σ_q(GeV/c)	α_s
x_p	Q_1	Q_2	0.722 ± .017	0.358 ± .003	0.209 ± .004
x_p	p_{Tout}	p_{Tin}	0.709 ± .012	0.356 ± .002	0.181 ± .003
x_p	L_1	L_2	0.722 ± .015	0.344 ± .003	0.185 ± .004
x_p	Q_1	ΔM^2	0.782 ± .020	0.357 ± .003	0.181 ± .006

Table 4b: Fit results for the string model, 1st order QCD (from TASSO[36]).

Distribution			a_L	σ_q(GeV/c)	α_s
x_p	Q_1	Q_2	0.484 ± .017	0.322 ± .004	0.288 ± .005
x_p	p_{Tout}	p_{Tin}	0.526 ± .012	0.337 ± .003	0.247 ± .004
x_p	L_1	L_2	0.431 ± .016	0.319 ± .004	0.292 ± .005
x_p	Q_1	ΔM^2	0.494 ± .021	0.325 ± .004	0.283 ± .009

Note, the errors given in Tables 4, 5 do not include systematic uncertainties.

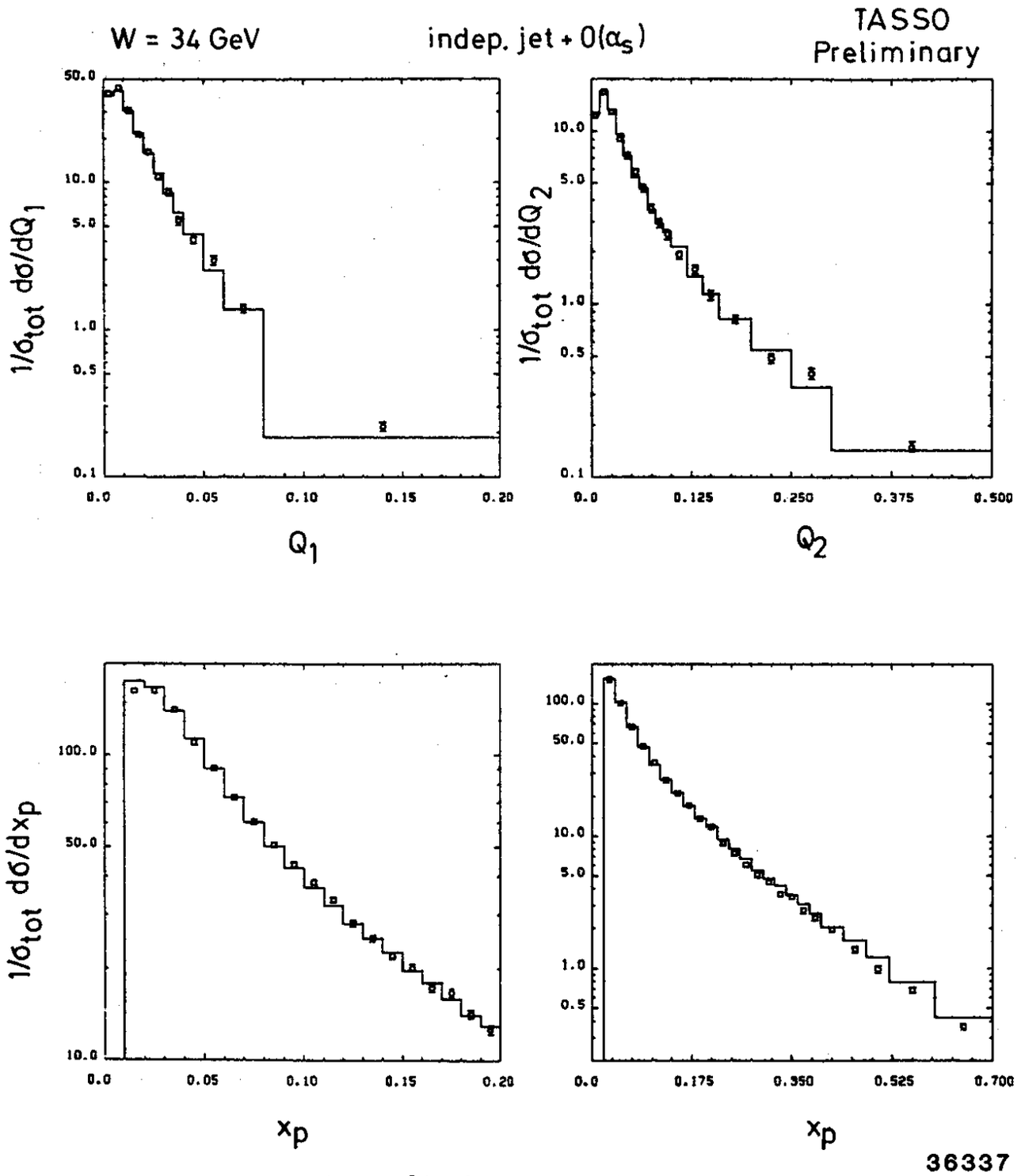

Fig.16 The corrected normalized cross sections for Q_1, Q_2 and x_p compared with QCD in $O(\alpha_s)$ using independent jet fragmentation. From TASSO, Ref. 36.

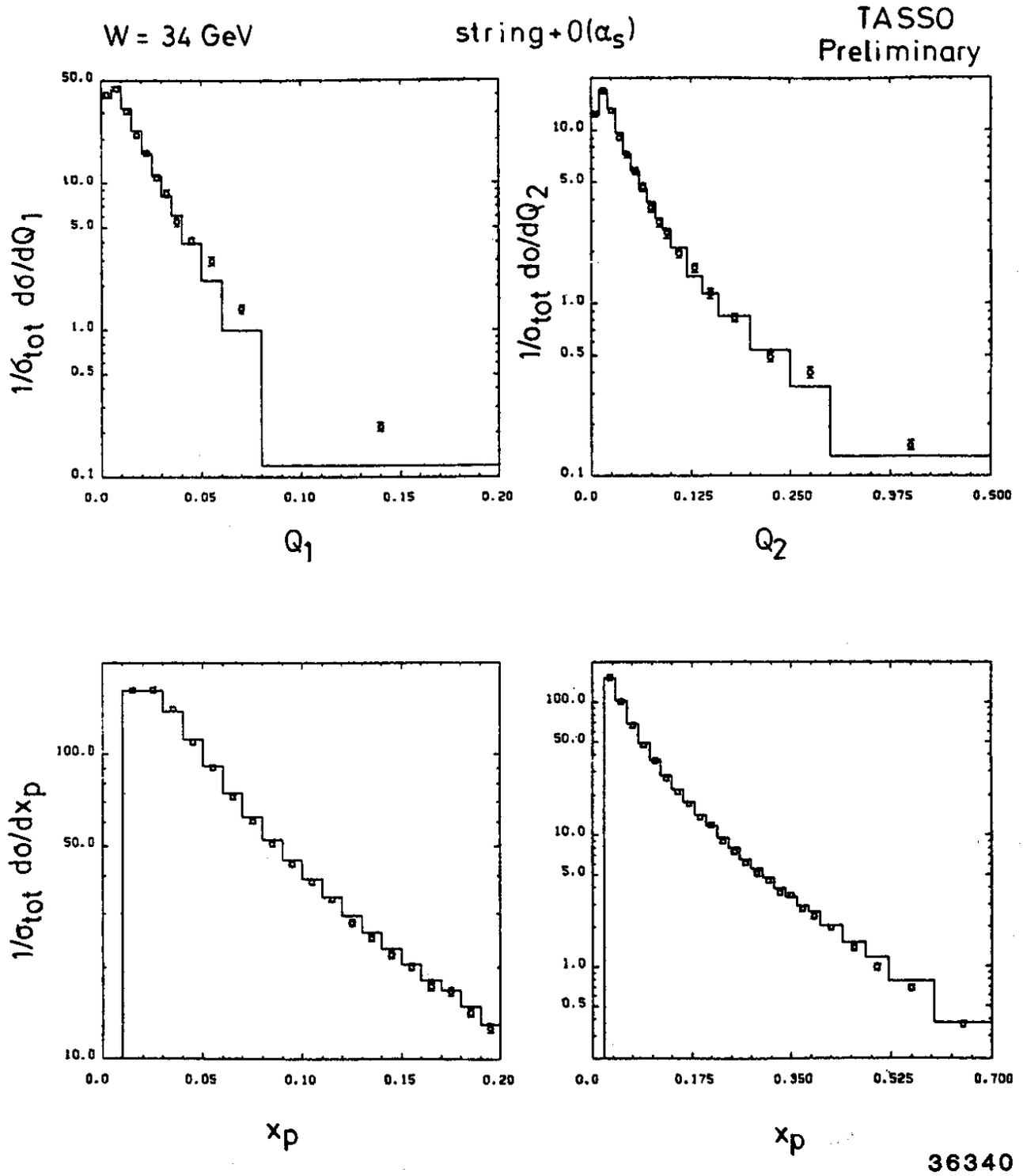

Fig.17 The corrected normalized cross sections for Q_1, Q_2 and x_p compared with QCD in $O(\alpha_s)$ using string fragmentation. From TASSO, Ref. 36.

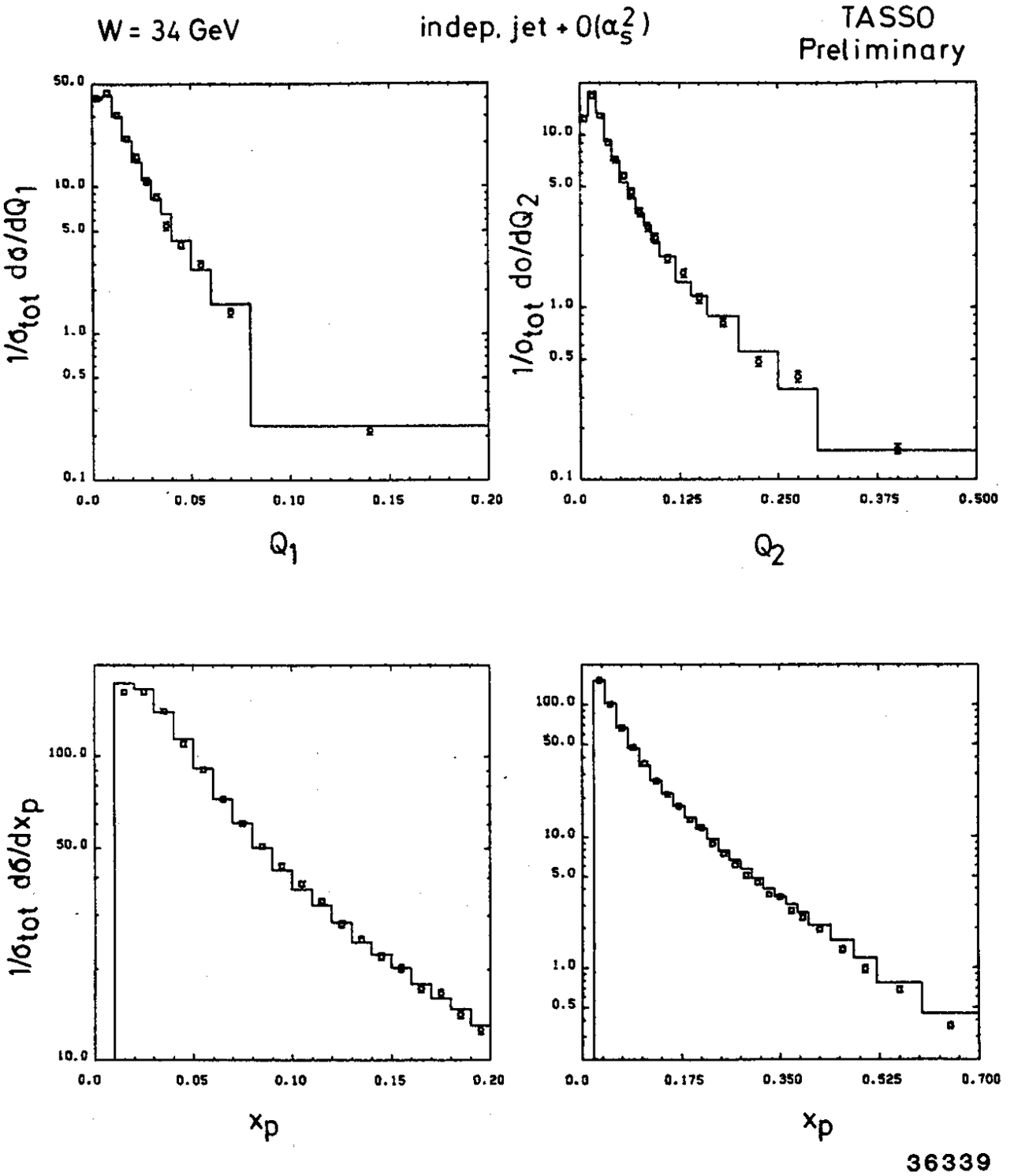

Fig.18 The corrected normalized cross sections for Q_1, Q_2 and x_p compared with QCD in $O(\alpha_s^2)$ using independent jet fragmentation. From TASSO, Ref. 36.

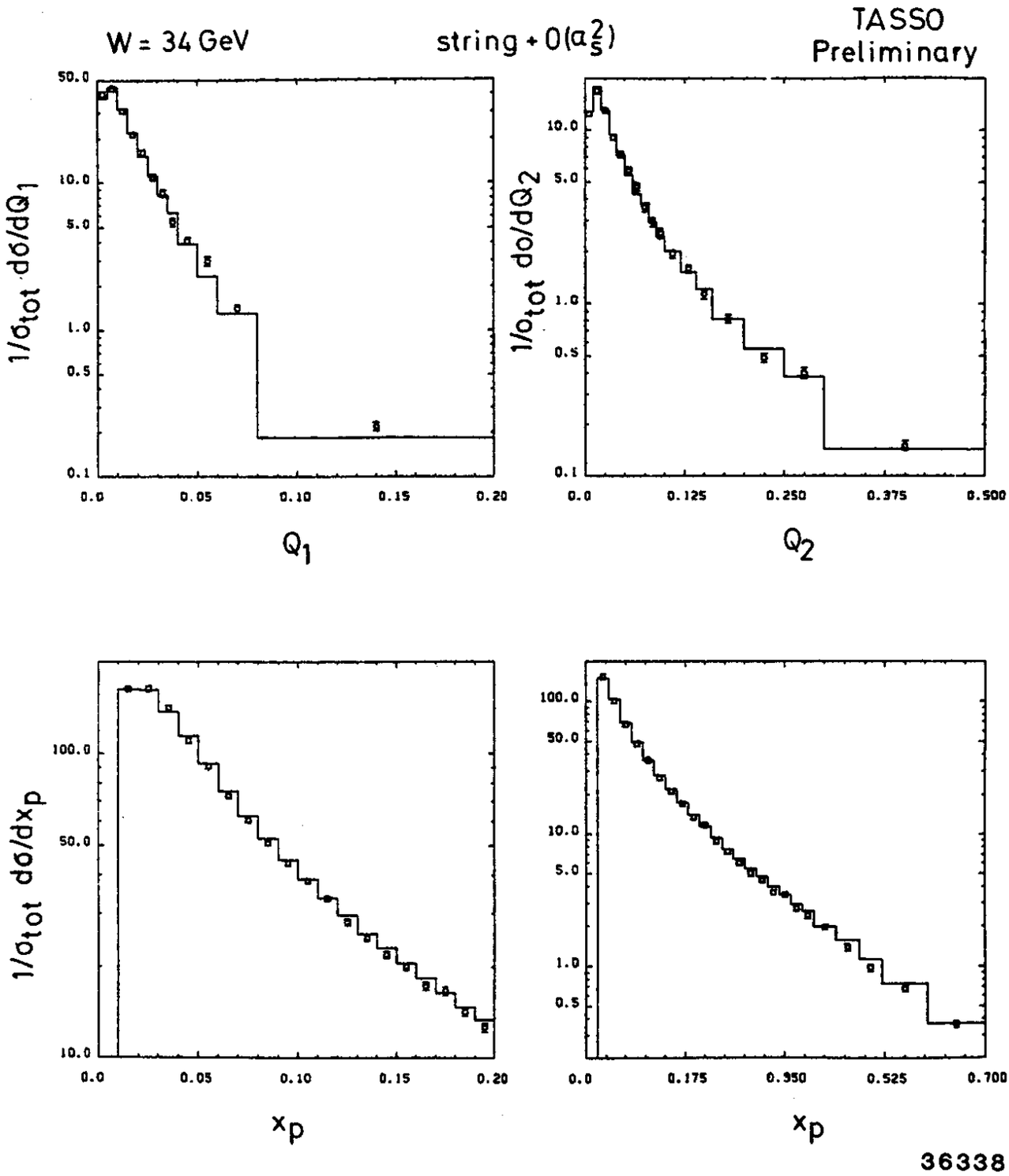

Fig.19 The corrected normalized cross sections for Q_1, Q_2 and x_p compared with QCD in $O(\alpha_s^2)$ using string fragmentation. From TASSO, Ref. 36.

Table 5a: Fit results for the independent jet model, 2nd order QCD (from TASSO[36]).

Distribution			a_L	σ_q(GeV/c)	α_s
x_p	Q_1	Q_2	0.687 ± .017	0.362 ± .003	0.166 ± .003
x_p	p_{Tout}	p_{Tin}	0.639 ± .014	0.350 ± .002	0.155 ± .002
x_p	L_1	L_2	0.697 ± .016	0.346 ± .003	0.155 ± .003
x_p	Q_1	ΔM^2	0.678 ± .020	0.355 ± .003	0.166 ± .004

Table 5b: Fit results for the string model, 2nd order QCD (from TASSO[36]).

Distribution			a_L	σ_q(GeV/c)	α_s
x_p	Q_1	Q_2	0.449 ± .017	0.326 ± .004	0.216 ± .003
x_p	p_{Tout}	p_{Tin}	0.473 ± .012	0.324 ± .003	0.201 ± .003
x_p	L_1	L_2	0.390 ± .016	0.323 ± .004	0.221 ± .003
x_p	Q_1	ΔM^2	0.437 ± .020	0.320 ± .004	0.219 ± .004

a) first order fits

Within each model the different combinations give consistent results for the fragmentation parameters. The value of σ_q is slightly smaller, $\sigma_q \sim 0.325$ GeV/c in the string model, compared to $\sigma_q \sim 0.355$ GeV/c in the independent jet model. The independent jet model yields $\alpha_s = 0.18 - 0.21$ while the string model yields 1.4 - 1.6 times larger values for α_s ($\alpha_s = 0.25 - 0.29$). This is in accord with the observations of the CELLO group. All distributions are well described by both models except for the tails of the Q_1 and $p_{T\ out}$ distributions where the string model predicts too few events. This discrepancy is removed in the second order fits (see Fig. 19).

b) second order fits

The fitted values for α_s in second order are 10 - 25 % smaller than in first order. The α_s values in the string model are 1.3 to 1.4 times higher than in the independent jet model.
These conclusions remain unchanged when the cutoff parameters ε,δ used in the QCD calculation of FKSS are varied, or when the gluon fragmentation scheme is changed. Furthermore, the cluster analysis performed in first order QCD leads to the same result. The best values found for α_s, and for the QCD parameter Λ deduced from it (in the two loop

approximation[44] are:

	independent jet model	string model
α_s	0.16 ± 0.015	0.21 ± 0.015
$\Lambda_{\overline{MS}}$	$0.42 \,^{+\,0.2}_{-\,0.15}$ GeV	1.3 ± 0.3 GeV

The errors given include the statistical and systematic uncertainties.

3.5 Some remarks on the determination of α_s from event shape mesures

Using FKSS the $O(\alpha_s^2)$ contribution is small. It is not known whether this conclusion changes when the terms of $O(\varepsilon,\delta)$ which have been neglected by FKSS are included.

The conclusion first drawn by the CELLO group that independent jet and string fragmentation yield different values for α_s seems unavoidable. The α_s value obtained in the independent jet model would probably be found also in many other fragmentation models provided quarks and gluons fragment independently and the model describes all relevant features of the data.

The cause for the significantly larger value of α_s deduced with the string model has been discussed in sect. 3.2: the directions of the final hadron jets differ from those of the original partons in a systematic way. The angle between the hadron jets of the gluon and the nearest quark are smaller than between gluon and quark. Hence, the string scheme makes qqg events to look more like two-jet events. As a result, α_s has to be increased in the string model in order to account for the observed number of three-jet events.

The generalizing statement made before on independent jet models can probably not be made for the string model. The Lund prescription for breaking the string is not the only possible and it is conceivable that another string model will yield significantly different fragmentation distributions.

One may ask whether the data permit a choice between the two fragmentation schemes. The JADE group[45] has made two observations which give some preference to the string model. They have investigated for planar events the particle distributions in the event plane. An excess of the particle yield in the region between quark and gluon jets compared to that between the two quark jets has been observed. A further clue comes from an analysis of the particle distribution around the jet axes. The events have been analyzed as three-jet events and each particle has been associated with one of the three-jets. The jets have been ordered such that jet 1 (jet 3) is opposite to the smallest (largest) angle. From QCD model calculations it is expected that for about half of the events jet 3 is the gluon jet. For each particle in a jet, p_T^{in}, the momentum component in the event plane transverse to the jet axis has been calculated, defining the sign of p_T^{in} as shown by the insert of Fig. 20. For each jet the average p_T^{in} has been determined as a function of the momentum component along the

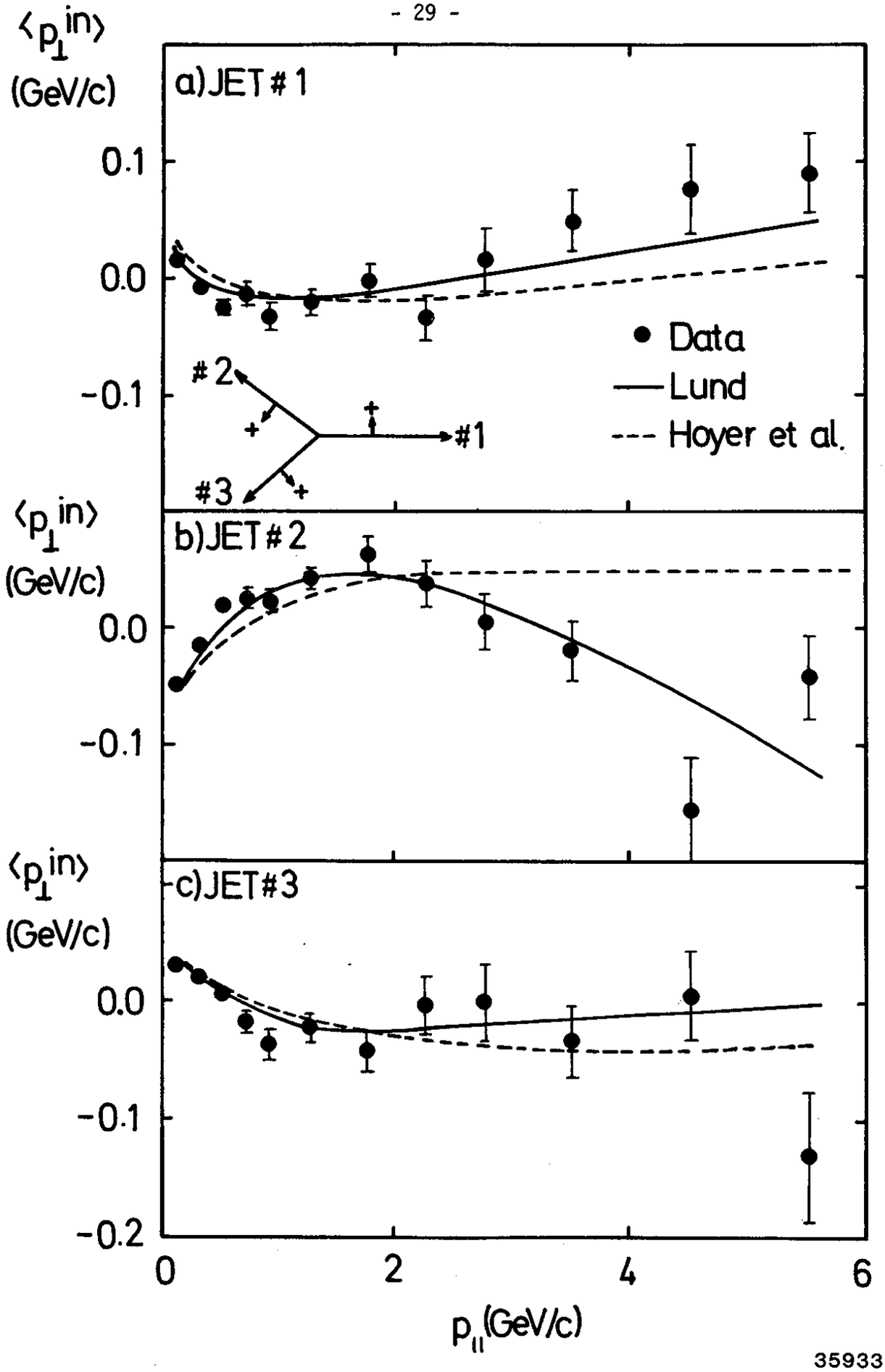

Fig.20 The average transverse momentum of charged particles in the event plane, $\langle p_{Tin} \rangle$, as a function of the momentum component parallel to the jet axis for the particles in jet 1, jet 2 and jet 3. The sign of p_{Tin} for each jet is defined by the insert. From JADE, Ref. 45.

jet axis (Fig. 20). For $p_{\mu} \gtrsim 3$ GeV/c $\langle p_T^{in} \rangle$ of jet 1 tends to be positive while $\langle p_T^{in} \rangle$ of jet 2 is negative. The string model (solid curves) reproduces that trend while the independent jet model (dashed curves) fails to describe the data. In the string model the low energy particles from the q and $\bar{q}$ jets are pulled by the Lorentz transformations towards the gluon jet while the fast particles are only little affected.

Since the particle momenta on average increase with increasing c.m. energy, at high energies the effects of the Lorentztransformations should be less important and the determination of α_s should become less dependent on the fragmentation scheme.

4. Energy-energy correlations

Energy-energy correlations have been proposed by Dokshitzer et al.[46] and Basham et al.[47] as a means to gain information on the parton angular distribution and in particular on the emission of hard as well as soft gluons. Consider two particles a and b emitted in the reaction

$$e^+e^- \rightarrow a + b + x$$

with fractional energies x_a and x_b ($x = 2E/W$) and angle χ between them (see Fig. 21). The energy weighted two-particle differential cross section reads

$$\frac{d\Sigma}{d\cos\chi} = \frac{1}{4\sigma_{tot}} \sum_{a,b} \int dx_a \, dx_b \, x_a \, x_b \, \frac{d^3\sigma}{dx_a dx_b \, d\cos\chi}$$

where σ is the total cross section. The summation is performed over all two-particle combinations including a = b (note: ab and ba are counted as two pairs). The normalization is such that $\int (d\Sigma/d\cos\chi) d\cos\chi = 1$. The theoretical premise has been that the cross section Σ determined with hadrons is equal to Σ evaluated with the partons (Fig. 22). In some calculations the soft gluon contribution is summed to all orders in the peaking approximation (i.e. all soft gluons are taken to be collinear) and interference terms - which might be important - are neglected. The hard noncollinear gluon emission is added by hand. It is assumed, that the transition from partons to hadrons occurs so late that the hadrons have approximately the same kinematics as the partons and that $d\Sigma/d\cos\chi$ is the same for hadrons and partons.

It is instructive to study $d\Sigma/d\cos\chi$ for some simple cases. In Fig. 23a the case $e^+e^- \rightarrow q\bar{q}$ is shown which would yield two δ functions at $\cos\chi = \pm 1$; finite resolution in λ, $\Delta = \Delta(\cos\chi)$, leads to $d\Sigma/d\cos\chi = (2\Delta)^{-1}$ at $1 > \cos\chi > 1 - \Delta$ and $-1 < \cos\chi < -1 + \Delta$. This result remains unchanged if the fragmentation process produces only collinear hadrons ($\sigma_q = 0$, Fig.23b). As long as the transverse momenta of the produced hadrons can be ignored the longitudinal momentum distribution

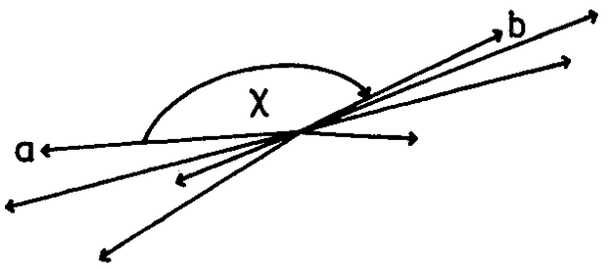

Fig.21 Definition of the angle χ

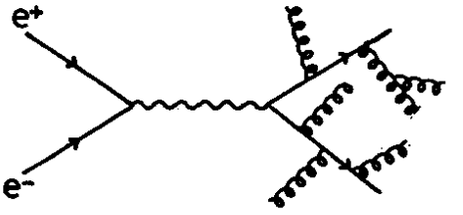

Fig.22 Multigluon emission diagram

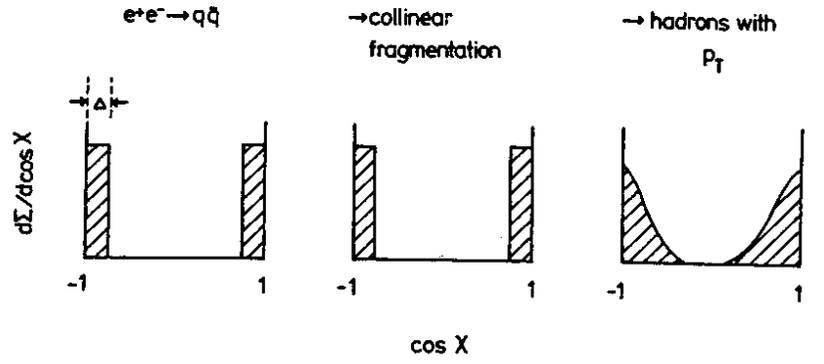

Fig.23 Illustration of energy-energy correlations for $e^+e^- \to q\bar{q}$.

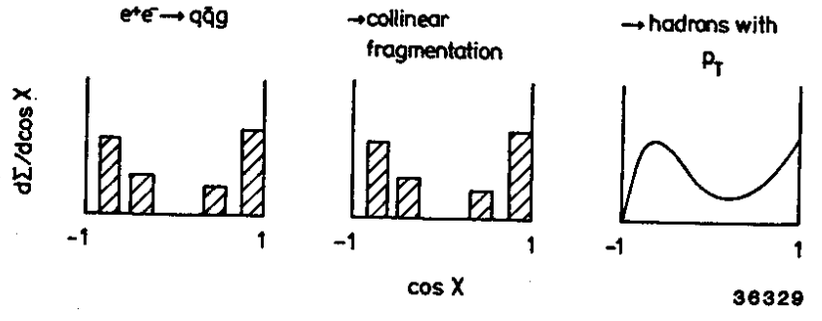

Fig.24 same as Fig.23 for $e^+e^- \to q\bar{q}g$.

does not affect $d\Sigma/d\cos\chi$ (e.g. whether 10 particles with $x = 0.1$ or 50 with $x = 0.02$ emerge has no effect). This is the virtue of the linear weighting with the energies x. The inclusion of transverse momenta produces a smearing of the forward and backward peaks (Fig. 23c).

Next we look at $e^+e^- \to q\bar{q}g$ with the gluon being emitted at a fixed angle and with fixed energy. The parton level distribution is shown in Fig. 24a. Outside the $\cos\chi = \pm 1$ regions there are three peaks corresponding to the three angles between the partons q, $\bar{q}$ and g. The hadron level distribution for collinear hadron emission is idential to it (Fig. 24b). The inclusion of transverse momentum produces the smeared distribution of Fig. 24c.

We have seen that fragmentation, in particular the transverse momentum distribution of hadrons, leads to significant differences for $d\Sigma/d\cos\chi$ between the partonic and hadronic levels. The effect of fragmentation, almost cancels for $e^+e^- \to q\bar{q}$ if, instead of $d\Sigma/d\cos\chi$ the difference of the "parallel" minus the "antiparallel" cross section, called the asymmetry, is considered[49]:

$$A(\chi) = \frac{d\Sigma}{d\cos\chi}(\pi - \chi) - \frac{d\Sigma}{d\cos\chi}(\chi) \qquad (19)$$

The asymmetry enhances the contribution from hard noncollinear gluon bremsstrahlung relative to the $q\bar{q}$ contribution and thereby increases the sensitivity to α_s. However, the asymmetry depends still on the fragmentation of gluons into hadrons. The parameters for gluon fragmentation cannot be determined from Σ or A but have to be found in some other way, e.g. from the shape analysis described in sect. 3.

The first analyses of Σ have been performed by the PLUTO group[50] for W's between 7 and 32 GeV. It has been found difficult to distinguish soft gluon contributions from fragmentation effects. The MARK II group[51] has analysed Σ as well as A at $W = 29$ GeV in an attempt to determine α_s (in first order QCD). Fig. 25 compares the measured asymmetry (corrected for detector and radiative effects, not corrected for acceptance) with the QCD prediction at the parton level (dashed curve) and the QCD plus fragmentation model result. With $\alpha_s = 0.19$ a good description of the data has been obtained but fragmentation effects limit the precision of the α_s measurement. The CELLO group[52] has analysed $A(\chi)$(Fig.25b) in first order QCD and found a sizeable difference in the values of α_s determined with independent jet fragmentation, $\alpha_s = 0.15 \pm 0.02$ and with string fragmentation, $\alpha_s = 0.25 \pm 0.04$. Note, these results are in accord with the event shape results of the same group. The MARK J group[53] has used the scheme of Ref. 54 to extract α_s from $A(\chi)$. The $O(\alpha_s^2)$ prediction has been calculated according to Ref. 54 where ε,δ-type cuts have been imposed on the ERT cross section formulae[19]. The (uncorrected) data are shown in Fig. 26 together with the QCD model prediction which includes fragmentation and detector effects. The values obtained for α_s are 0.12 ± 0.01 (independent jet) and 0.14 ± 0.01 (string). This result is puzzling. It seems to be at

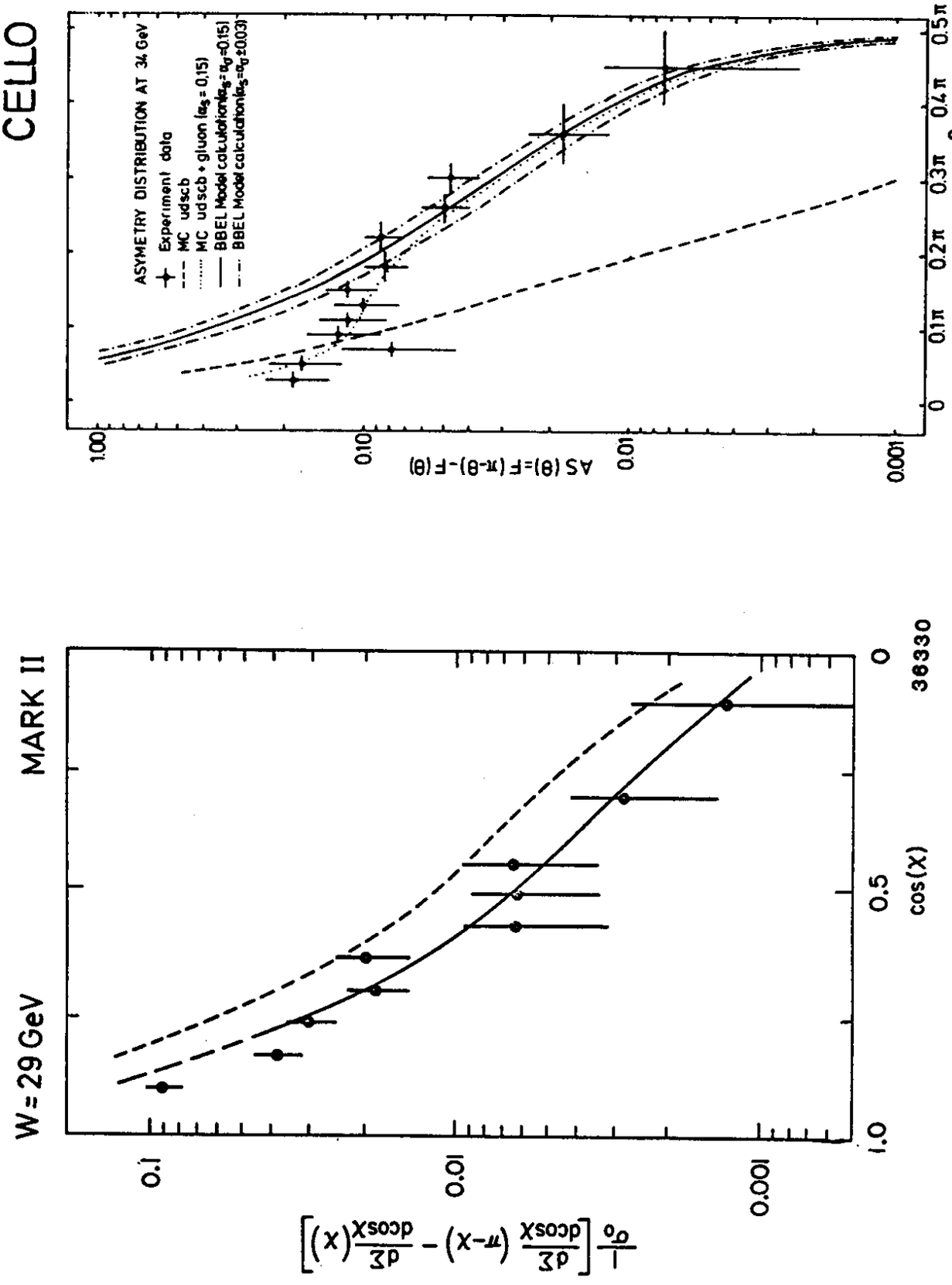

Fig.25 The asymmetry A(X) compared with QCD models a) MARK II (Ref. 51), not corrected for acceptance, dashed curve gives QCD prediction at the parton level, solid curve includes fragmentation b) CELLO, Ref. 52, corrected data compared to various QCD models.

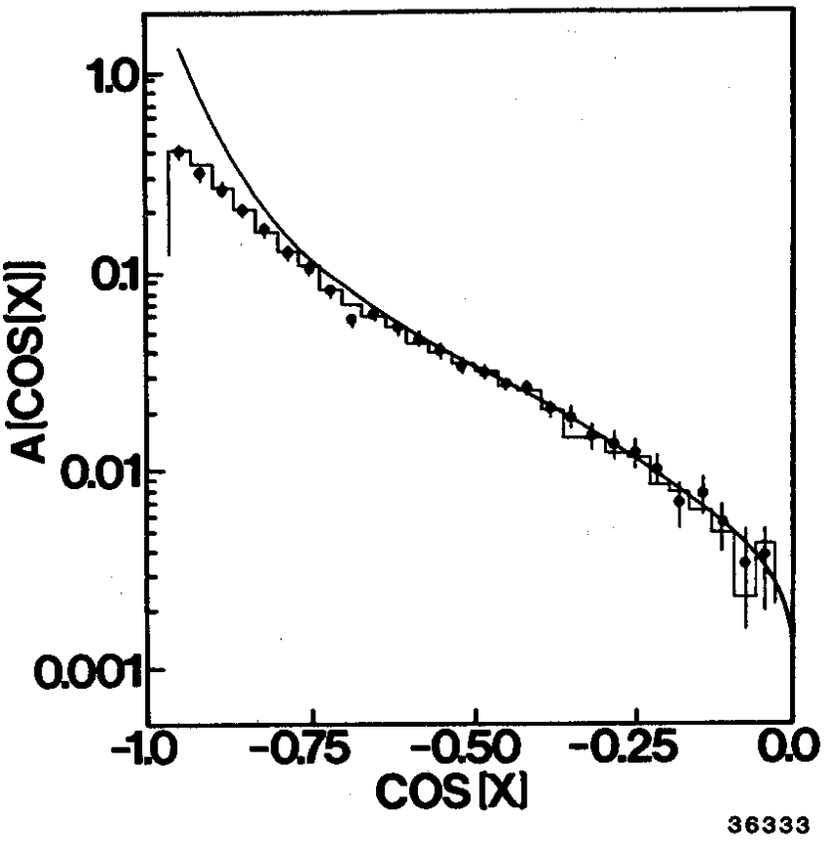

Fig.26 The (uncorrected) asymmetry compared with a QCD model prediction in $O(\alpha_s^2)$. From MARK J, Ref. 53.

variance with the α_s values obtained by the same group from shape analyses (see Table 2). It is also in disagreement with the α_s values obtained in $O(\alpha_s^2)$ by TASSO from event shapes, viz. α_s (independent jet) = 0.16 ± 0.015 and α_s (string) = 0.21 ± 0.015.

The solution to this puzzle is unknown. Barring any experimental problems it could indicate an inconsistency of QCD in the sense, that the energy-energy correlations and event shapes, which test different configurations in phase space require different α_s values to fit the data. However, preliminary data from the TASSO group indicate that in $O(\alpha_s^2)$ the α_s value determined from event shapes fits also $A(\chi)$. The different procedures used to calculate QCD in $O(\alpha_s^2)$ could also be at the origin of the discrepancy. It has been pointed out by Ref. 54 that terms of $O(y^{1/2})$ and $O(\varepsilon,\delta)$ which have been omitted in the FKSS calculation might not be negligible. On the other hand, it seems unclear whether the procedure used by Ref. 54 does or does not include contributions from kinematic areas where higher order (beyond $O(\alpha_s^2)$ terms) are important.

In summary, it appears premature to deduce a precise value of α_s from energy-energy correlation studies.

5. Conclusion

The extraction of α_s from hadron production by e^+e^- annihilation appears to encounter a new uncertainty principle which requires the product of experimental precision and theoretical uncertainty to be large. Where the theory is well defined such as for $R = \sigma_{tot}/\sigma_{\mu\mu}$, the experiments have difficulties to achieve the desired accuracy. The value of α_s deduced near W = 34 GeV in $O(\alpha_s^2)$ is $\alpha_s = 0.19 \pm 0.06$. The error is dominated by experimental uncertainties. Accurate data are available for two- and three-jet production. Here the precision of α_s is limited by the lack of a theory for fragmentation. The range of α_s values allowed by the data in $O(\alpha_s^2)$ near W = 34 GeV is $\alpha_s = 0.15$-0.22. To do better presumably requires a theoretical understanding of hadronization and/or data at higher c.m. energies.

Acknowledgements

Numerous discussions with G. Rudolph have been extremely valuable for the preparation of this talk. I am also indebted for discussions with G.Kramer, H.Kowalski and T.Sjöstrand. I want to thank J.Gunion for a most enjoyable meeting. I am very grateful to Mrs. E. Hell for her effort to get the manuscript ready.

References

1. see G.P.Lepage, 1983 Int.Symp. Lepton Photon Interact. at High Energies, Cornell.
2. see W.Wagner, this meeting and TH-Aachen Report PITHA 83/17 (1983)
3. F.A.Berends, R.Kleiss, Nucl.Phys. B177 (1981) 237; B178 (1981) 141.
4. M.Dine, J.Sapirstein, Phys.Rev.Lett. 43 (1979) 668;
   K.G.Chetyrkin, A.L.Kataev, F.V.Tkachev, Phys.Lett. 85B (1979) 277;
   W.Celmaster, R.J.Gonsalves, Phys.Rev.Lett. 44 (1979) 560.
5. J.Ellis and M.K.Gaillard, Physics with very High Energy e^+e^- colliding beams, CERN Report 76-18 (1976);
   J.Jersak, E.Laermann, P.M.Zerwas, Phys.Lett. 99B (1981) 363.
6. J.Schwinger, Particles, Sources and Fields (1973) Vol.II, New York, Addison-Wesley.
   Th.Appelquist, H.D.Politzer, Phys.Rev. D12 (1975) 1404.
7. TASSO Collaboration, R.Brandelik et al., Phys.Lett. 113B (1982) 499;
   MARK-J Collaboration, data reported by J.D.Burger, 21st Int.Conf. High Energy Physics, Paris (1982), ed. P.Petiau, M.Porneuf, C3-63;
   MAC Collaboration and MARK-II Collaboration, data reported by R.Hollebeek, SLAC-PUB-2989 (1982);
   JADE Collaboration, W.Bartel et al., Phys.Lett. 129B (1983) 145.
8. TASSO Collaboration, R.Brandelik et al., Phys.Lett. 86B (1979) 243;
   MARK-J Collaboration, D.P.Barber et al., Phys.Rev.Lett. 43 (1979) 830;
   PLUTO Collaboration, Ch.Berger et al., Phys.Lett. 86B (1979) 418;
   JADE Collaboration, W.Bartel et al., Phys.Lett 91B (1980) 142.
9. A.M.Polyakov, Proc. 7th Int.Symp. Lepton Photon Interactions High Energies, Stanford, 1975, p. 855.
10. J.Ellis, M.K.Gaillard, G.G.Ross, Nucl.Phys. B111 (1976) 253;
    T.A.De Grand, Y.G.Ng, S.H.H.Tye, Phys.Rev. D16 (1977) 3251;
    G.Kramer, G.Schierholz, I.Willrodt, Phys.Lett. 79B (1978) 249.
11. P.Hoyer et al., Nucl.Phys. B161 (1979) 34.
12. B.Andersson, G.Gustafson, T.Sjöstrand, Phys.Lett. 94B (1980) 211, and references quoted therein.
13. TASSO Collaboration, R.Brandelik et al., Phys.Lett. 97B (1980) 453;
    PLUTO Collaboration, Ch.Berger et al., Phys.Lett. 97B (1980) 459;
    CELLO Collaboration, H.J.Behrend et al., Phys.Lett. 110B (1982) 329.
14. T.A.Grand, Y.G.Ng, S.H.H.Tye, Phys.Rev. D16 (1977) 3251.
15. P.Söding, DESY Report 81-070 (1981).
16. G.Preparata, G.Valenti, Nucl.Phys. B183 (1981) 53;
    L.Angelini et al., Univ. of Bari, Bari GT 82-12. 82-14 (1982).
17. M.G.Bowler, Oxford University, Nucl.Phys.Lab. Report 106/81 (1981).
18. A.Ali et al., Phys.Lett. 93B (1980) 155; Nucl.Phys. B167 (1980) 454.
19. R.K.Ellis, D.Ross, A.Terrano, Phys.Lett. 45B (1980) 1226; Nucl. Phys. B178 (1980) 421.
20. K.Fabricius, G.Kramer, G.Schierholz, I.Schmitt, Phys.Lett. 97B (1980) 431; Z.Phys. C11 (1982) 315.
21. J.Vermaseren, J.Gaemers, S.Oldham, Nucl.Phys. B187 (1981) 301.
22. G.Sterman, S.Weinberg, Phys.Rev.Lett. 39 (1977) 1436.
23. T.Gottschalk, Phys.Lett. 109B (1982) 331.
24. G.Kramer, DESY Report 83-068 (1983).
25. R.D.Field, R.P.Feynman, Nucl.Phys. B136 (1978) 1.

26. J.B.Babcock, R.E.Cutkosky, Carnegie-Mellon Univ. Report COO-3066-144 (1980);
K.Lanius et al., Z.Phys. C8 (1981) 251;
H.J.Daum, H.Meyer, J.Bürger, Z.Phys. C8 (1981) 167;
J.Dorfan, Z.Phys. C7 (1981) 349.
27. J.D.Bjorken, S.Brodsky, Phys.Rev. D1 (1970) 1416.
28. L.Clavelli, H.P.Nilles, Phys.Rev. D21 (1980) 1242;
L.Clavelli, Preprint ANL-HEP-CP-83-05 (1983).
29. MARK-J Collaboration, D.P.Barber et al., Phys.Lett. 89B (1979) 139.
30. H. Newman, Proc. 20th Int.Conf. High Energy Physics, Madison (1980).
31. TASSO Collaboration, R.Brandelik et al., Phys.Lett. 94B (1980) 437.
32. JADE Collaboration, W.Bartel et al., Phys.Lett. 91B (1980) 142;
S.Yamada, Proc. 20th Int.Conf. High Energy Physics, Madison (1980).
33. PLUTO Collaboration, Ch.Berger et al., Phys.Lett. 97B (1980) 459.
34. CELLO Collaboration, H.J.Behrend et al., Nucl.Phys. B218 (1983) 269.
35. JADE Collaboration, W.Bartel et al., Phys.Lett. 119B (1982) 239.
36. TASSO Collaboration, data reported by G.Rudolph at the EPS Int.Conf. High Energy Physics, Brighton (1983).
37. C.Peterson et al., Phys.Rev. D27 (1982) 77.
38. TASSO Collaboration, M.Althoff et al., Phys.Lett. 126B (1983) 493.
39. MARK II Collaboration, data reported by
G.Trilling, 21st Int.Conf High Energy Physics, Paris (1982), ed. P.Petiau, M.Porneuf;
M.E.Nelson et al., SLAC-PUB-3059 (1983).
40. TASSO Collaboration, R.Brandelik et al., Phys.Lett. 117B (1982) 135.
41. TASSO Collaboration, R.Brandelik et al., Phys.Lett. 105B (1981) 75;
M.Althoff et al., Z.Phys. C17 (1983) 5.
42. TASSO Collaboration, M.Althoff et al., DESY Report 83-071 (1983).
43. T.Meyer, Z.Phys. C12 (1982) 77.
44. W.Caswell, Phys.Rev.Lett. 33 (1974) 244;
D.R.T.Jones, Nucl.Phys. B75 (1974) 531.
45. JADE Collaboration, W.Bartel et al., DESY Report 83-079 (1983).
46. Y.L.Dokhshitzer, D.I.D'Yakonov, S.I.Troyan, Phys.Lett. 78B (1978) 290; Phys.Rev. 58 (1980) 269.
47. C.L.Basham et al., Phys.Rev.Lett. 41 (1978) 1585; Phys.Rev. D19 (1979) 2018.
48. A.Bassetto, M.Ciafaloni, G.Marchesini, Phys.Lett. 83B (1978) 207;
K.Konishi, Rutherford Report RL 97-035 (1979);
W.Furmanski, S.Pokorski, Nucl.Phys. 155B (1979) 253;
A.H.Müller, Phys.Lett. 104B (1981) 161;
Columbia University Reports CU-TP-247 (1982) and CU-TP-249 (1982).
49. C.L.Basham et al., Phys.Rev. D24 (1981) 2383.
50. PLUTO Collaboration, Ch.Berger et al., Phys.Lett. 90B (1980) 312; 99B (1981) 292.
51. D.Schlatter et al., Phys.Rev.Lett. 49 (1982) 521.
52. CELLO Collaboration, H.J.Behrend et al., Z.Phys. C14 (1982) 95.
53. MARK-J Collaboration, D.P.Barber et al., Phys.Rev.Lett. 50 (1983) 2051.
54. A.Ali, F.Barreiro, Phys.Lett. 118B (1982) 155; DESY Report 83-070 (1983).